

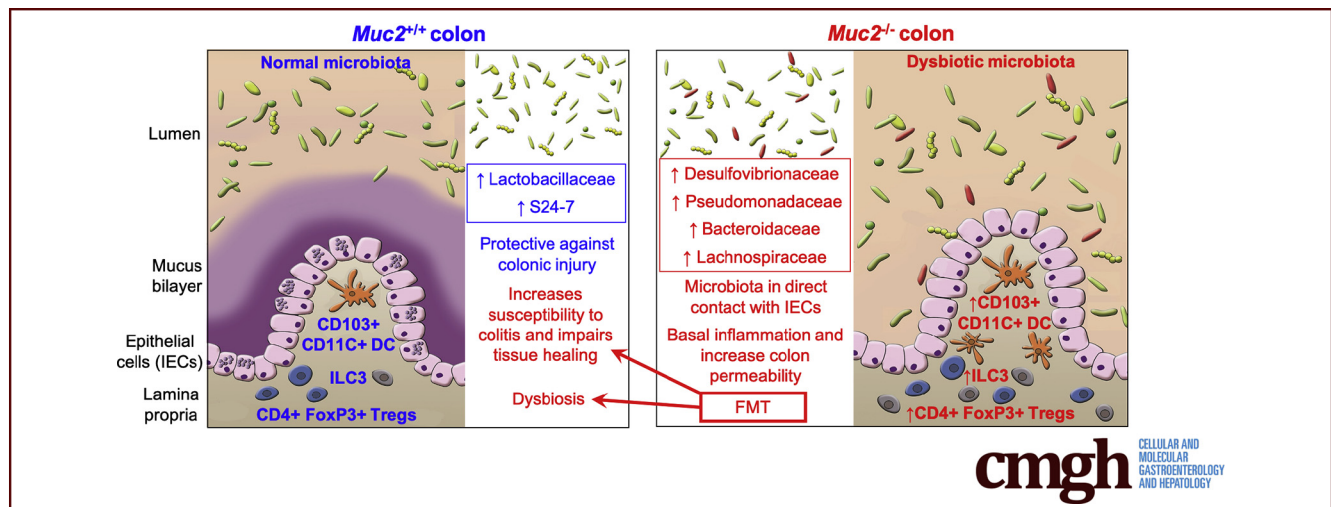
ORIGINAL RESEARCH

Muc2 Mucin and Nonmucin Microbiota Confer Distinct Innate Host Defense in Disease Susceptibility and Colonic Injury



Aralia Leon-Coria,^{1,*} Manish Kumar,^{1,*} Matthew Workentine,² France Moreau,¹ Michael Surette,^{1,3} and Kris Chadee¹

¹Department of Microbiology, Immunology and Infectious Diseases, University of Calgary Health Sciences Centre, Calgary, Alberta, Canada; ²Department of Veterinary Medicine, University of Calgary, Calgary, Alberta, Canada; and ³Department of Biochemistry and Biomedical Sciences, McMaster University, Hamilton, Ontario, Canada



SUMMARY

This study interrogates the impact of alterations in the microbial composition in animals with and without Muc2 mucin in colonic epithelial barrier dysfunction and inflammation. The absence of a protective mucus barrier alters microbiota to promote inflammation and intestinal permeability.

BACKGROUND & AIMS: Alterations in intestinal MUC2 mucin and microbial diversity are closely linked with important intestinal pathologies; however, their impact on each other and on intestinal pathogenesis has been vaguely characterized. Therefore, it was of interest in this study to delineate distinct and cooperative function of commensal microbiota and the Muc2 mucin barrier in maintaining intestinal epithelial barrier function.

METHODS: Muc2 mucin deficient (*Muc2*^{-/-}) and sufficient (*Muc2*^{+/+}) littermates were used as a model for assessing the role of Muc2. To quantify the role of the microbiota in disease pathogenesis, *Muc2*^{+/+} and *Muc2*^{-/-} littermates were treated with a cocktail of antibiotics that reduced indigenous bacteria, and then fecal transplanted with littermate stool and susceptibility to dextran sulphate sodium (DSS) quantified.

RESULTS: Although, *Muc2*^{+/+} and *Muc2*^{-/-} littermates share similar phyla distribution as evidenced by 16S sequencing they maintain their distinctive gastrointestinal phenotypes. Basally, *Muc2*^{-/-} showed low-grade colonic inflammation with high populations of inflammatory and tolerogenic immune cells that became comparable to *Muc2*^{+/+} littermates following antibiotic treatment. Antibiotics treatment rendered *Muc2*^{+/+} but not *Muc2*^{-/-} littermates highly susceptible to DSS-induced colitis that was ILC3 dependent. *Muc2*^{-/-} microbiota was colitogenic to *Muc2*^{+/+} as it worsened DSS-induced colitis. Microbiota dependent inflammation was confirmed by bone-marrow chimera studies, as *Muc2*^{-/-} receiving *Muc2*^{+/+} bone marrow showed no difference in their susceptibility toward DSS induced colitis. *Muc2*^{-/-} microbiota exhibited presence of characteristic OTUs of specific bacterial populations that were transferrable to *Muc2*^{+/+} littermates.

CONCLUSIONS: These results highlight a distinct role for Muc2 mucin in maintenance of healthy microbiota critical in shaping innate host defenses to promote intestinal homeostasis. (*Cell Mol Gastroenterol Hepatol* 2021;11:77-98; <https://doi.org/10.1016/j.jcmgh.2020.07.003>)

Keywords: Muc2; Microbiota; Colitis; Dysbiosis; Mucus.

A diverse population of microorganisms, collectively called the “gut microbiota,” have adapted to live symbiotically in/on the intestinal mucus surface¹ and play a critical role in host nutrition² and immune modulation.³ Their effects are largely dependent on complex interactions with host immune cells, and any imbalance could result in the development of disease. It has been estimated that approximately 100 billion bacteria of around 500–1000 species,^{2,4} encompassing 7–9 phyla,⁵ are present in the human gut. This huge diversity of gut microbiota largely dictates the outcome of host-microbiota interactions, as revealed by 16S rRNA sequencing and metagenomic analysis of healthy and inflammatory bowel disease (IBD) patients.⁶ Although genetic and environmental factors largely determine gut microbial diversity, 90% of gut bacteria belong to the phyla Firmicutes and Bacteroidetes in healthy individuals.⁷ However, some IBD patients have reduced biodiversity (alpha diversity) with a concomitant rise in pathobionts resulting in impaired activation of the host immune system.^{8–10} Even though a reduction in Firmicutes and rise in Proteobacteria is consistently seen in IBD patients, there is no direct causal association between specific pathogens and the development of IBD.^{11,12}

The intestinal mucus layer is formed of polymeric sheets of densely glycosylated MUC2 mucin.¹³ Depletion of the mucus layer is one of the most common characteristics in IBD patients, allowing gut microbial components to come in close contact with host cells and to elicit unregulated inflammation.¹⁴ A higher number of adherent-invasive *Escherichia coli* isolates have been observed in rectal biopsies from IBD patients.¹⁵ However, it is uncertain whether depletion of the mucus layer is a risk factor or a result of colonic inflammation in IBD patients.¹⁶ Findings by us and others have reaffirmed the importance of the mucus layer in maintaining homeostasis between gut microbiota and the host immune system.^{16–18} Recent studies have suggested specific groups of bacteria and their metabolites may have potent immune-modulatory effects on the host immune system.¹⁹ Thus, any alteration in microbial dynamics can predispose the host toward aggravated disease. Even though there is ample evidence to verify the close association of microbiota and the mucus layer in IBD pathogenesis, the exact role of each other on events responsible for the initiation and course of IBD is not clear. We hypothesize that these 2 factors, separately or together, can aggravate colonic inflammation to predispose the host toward IBD. Here we used *Muc2*^{+/+} and *Muc2*^{-/-} littermates to highlight the impact of the mucus layer on gut microbial dynamics and their collective influence in maintaining homeostasis between gut microbiota and host immune system.

Results

Muc2^{-/-} Littermates Exhibit Differential Gut Bacterial Composition That Drives Constitutive Colonic Inflammation

To normalize microbiota in both genotypes, littermates were generated using wild-type (WT) and in-house *Muc2*^{-/-}

animals. Characterization of their microbial compositions by 16s rRNA sequencing showed that *Muc2*^{+/+} and *Muc2*^{-/-} littermates had similar bacterial distribution, with no differences at the phyla level (Figure 1A, lanes a and c). Both genotypes included the phyla Firmicutes, Bacteroidetes, Tenericutes, Proteobacteria, and Actinobacteria in similar proportions. Furthermore, alpha diversity analysis showed similar species richness (Figure 1B); however, beta diversity analysis revealed distinct species diversity among the littermates (Figure 1C).

Muc2^{-/-} mice consistently develop mild colitis that culminated in rectal prolapse around 5 months of age and are highly susceptible toward chemical, bacterial, and parasite-induced colitis.^{20–22} Thus, to investigate the role of microbiota in disease pathogenesis, *Muc2*^{+/+} and *Muc2*^{-/-} littermates were treated with a broad-spectrum antibiotic cocktail,²³ and colonic proinflammatory cytokines transcript levels were analyzed. After antibiotic treatment, *Muc2*^{+/+} and *Muc2*^{-/-} littermates showed a shift in bacterial population and diversity, characterized by a decrease in Firmicutes, an absence of Bacteroidetes, and an increase in Proteobacteria phyla (Figure 1A, lanes b and d). Under basal conditions, *Muc2*^{-/-} expressed significantly higher levels of *Tnf-α* and *Il-1β* transcripts that were attenuated following antibiotics treatment (Figure 1D). To quantify whether high basal levels of proinflammatory cytokines were driving alterations in epithelial barrier function, intestinal permeability was assessed using fluorescein isothiocyanate (FITC) dextran. As predicted, basally *Muc2*^{-/-} showed increased intestinal permeability that was attenuated following antibiotics treatment (Figure 1E). Based on these findings and knowing that proinflammatory cytokines can alter tight junction (TJ) permeability,²⁴ we measured TJ expression in untreated and antibiotic-treated mice. *Muc2*^{-/-} showed decreased *Occludin* and *Claudin 2* basal expressions that were significantly increased (restored) to basal *Muc2*^{+/+} levels following antibiotic treatment (Figure 1F). These results suggest that *Muc2* mucin deficiency altered gut microbial composition that promoted colonic proinflammatory responses.

To assess if colonic bacteria were directly involved in eliciting colonic proinflammatory responses and alterations in TJ proteins, we visualized bacteria using fluorescent in situ hybridization. In *Muc2*^{+/+}, the intact mucus layer physically separating epithelial cells and colonic microbiota is evident, whereas in *Muc2*^{-/-} littermates, bacteria were in

*Authors share co-first authorship.

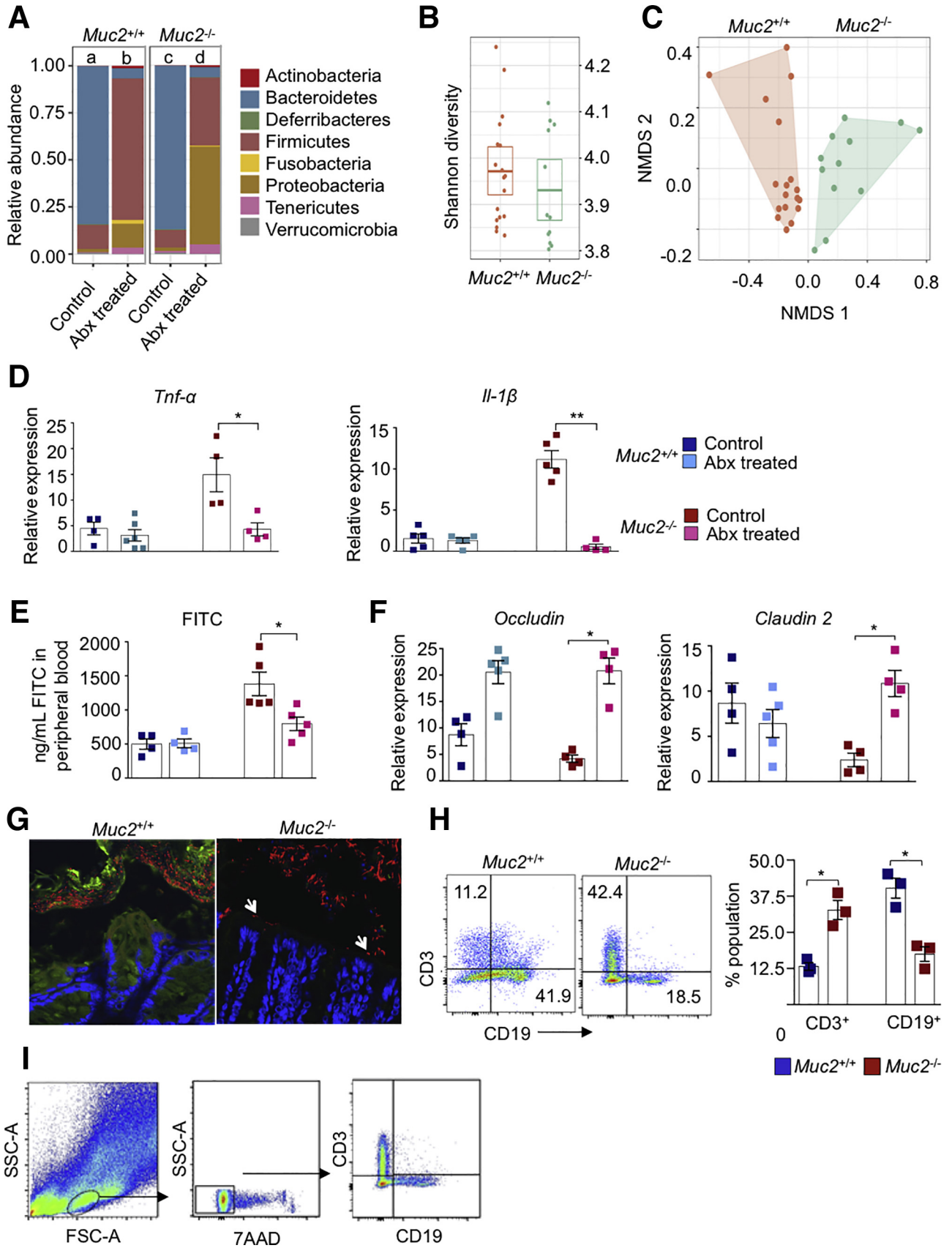
Abbreviations used in this paper: CDNA, complementary DNA; DAI, disease activity index; DSS, dextran sodium sulfate; FITC, fluorescein isothiocyanate; FMT, fecal microbiota transplantation; IBD, inflammatory bowel disease; IL, interleukin; ILC, innate lymphoid cell; LPL, lamina propria lymphocyte; mRNA, messenger RNA; PICRUST, phylogenetic investigation of communities by reconstruction of unobserved states; TGF-β, transforming growth factor β; TJ, tight junction; WT, wild-type.

 Most current article

© 2020 The Authors. Published by Elsevier Inc. on behalf of the AGA Institute. This is an open access article under the CC BY-NC-ND license (<http://creativecommons.org/licenses/by-nc-nd/4.0/>).

2352-345X

<https://doi.org/10.1016/j.jcmgh.2020.07.003>



direct contact with the colonic epithelium (arrows, Figure 1G). Host cells present in the mucosa recognize microbial products or their components via pattern recognition receptors²⁵ to facilitate recruitment of immune cells thereby regulating normal gut microbiota and immune system homeostasis.²⁶ Thus, to assess if gut bacteria in contact with the epithelium caused the recruitment of immune cells, immune phenotyping was done using lamina propria lymphocytes (LPLs). We chose to investigate adaptive immunity (B and T cells), as they are responsible for microbiota-specific immune responses and are mainly responsible to maintain gut microbiota composition.²⁷ We observed significantly higher CD3⁺ T cell and lower CD19⁺ B cell populations in the colon of *Muc2*^{-/-} as compared with *Muc2*^{+/+} littermates (Figure 1H; gating strategy is shown in Figure 1I). Taken together, these results demonstrate that the absence of a mucus barrier supports the growth of bacteria that could potentially drive colonic inflammation and recruit immune cells at the site of injury.

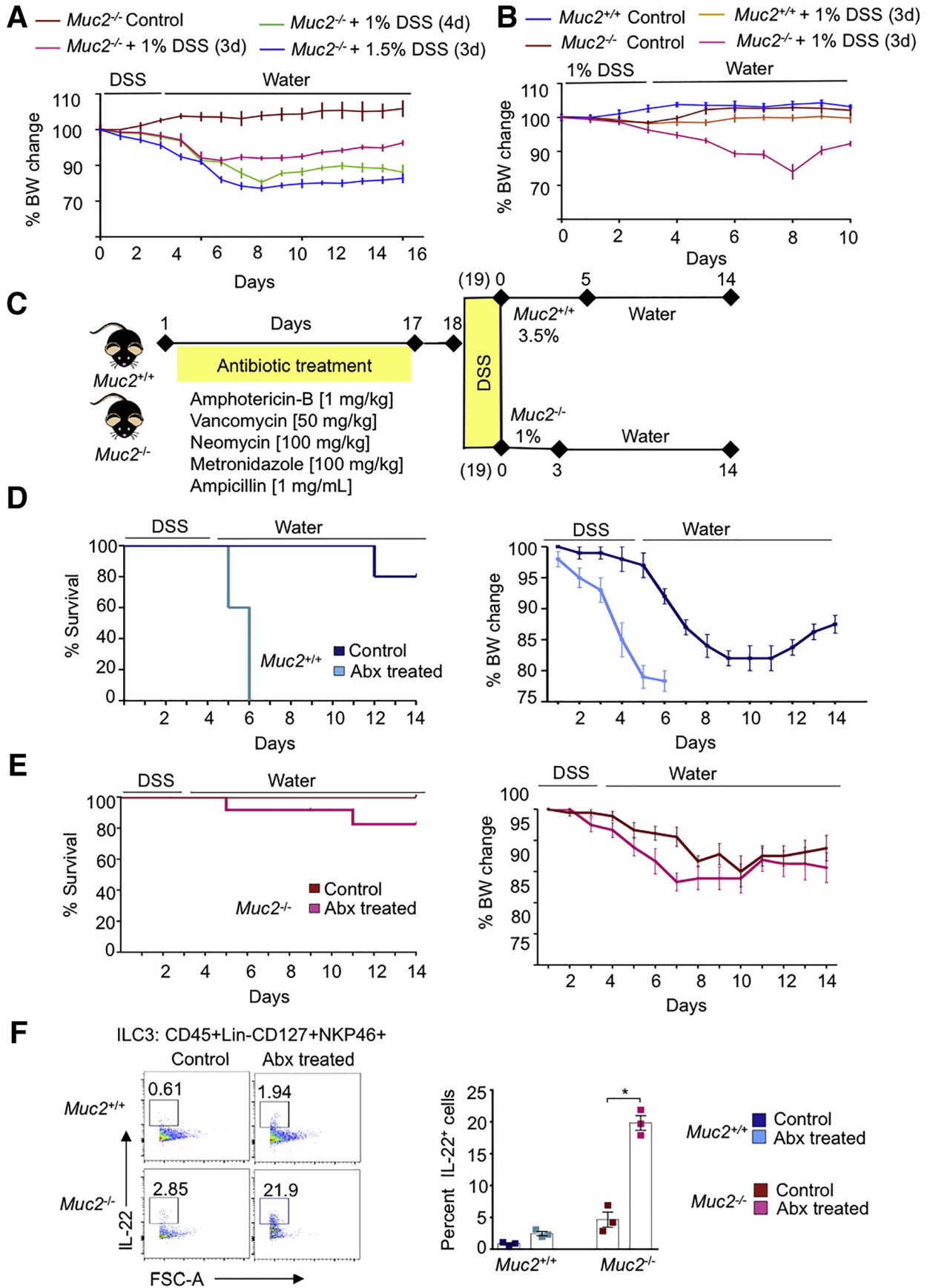
Muc2^{+/+} But Not *Muc2*^{-/-} Microbiota Is Required for Protection Against Dextran Sodium Sulfate-Induced Colitis

We next interrogated if mucus-associated (*Muc2*^{+/+}) and non-mucus-associated (*Muc2*^{-/-}) colonic microbiota played a protective role in susceptibility and resolution of dextran sodium sulfate (DSS)-induced colitis. We have previously shown¹⁷ that *Muc2*^{-/-} littermates are highly sensitive to DSS-induced colitis associated with high mortality and with a dosage of 1% DSS given orally for 3 days followed by water induced comparable weight loss and disease activity index (DAI) scores as *Muc2*^{+/+} receiving 3.5% DSS for 5 days. Based on these findings, we tested 3 different DSS treatment regime in *Muc2*^{-/-} to quantify disease susceptibility: (1) 1% DSS for 3 days, (2) 1% DSS for 4 days, and (3) 1.5% DSS for 3 days followed by water. *Muc2*^{-/-} given 1% DSS for 3 days lost 10% weight and slowly regained their weight up to 15 days. In

comparison, *Muc2*^{-/-} treated with 1% DSS for 4 days or 1.5% DSS for 3 days lost 20% of their body weight by day 8 and did not recover their weight up to 15 days (Figure 2A). Predictably, *Muc2*^{+/+} littermates given 1% DSS for 3 days followed by water up to 10 days did not lose body weight, as was similar to the water control animals (Figure 2B). Thus, to induce equivalent levels of inflammation-driven weight loss in both genotypes, for all subsequent studies, *Muc2*^{-/-} were treated with 1% DSS for 3 days and *Muc2*^{+/+} with 3.5% DSS for 5 days (see experimental regime in Figure 2C).

To investigate whether microbiota from *Muc2*^{+/+} and *Muc2*^{-/-} littermates conferred differential protective effects against colonic damage, animals were treated with antibiotics and challenged with DSS (Figure 2C). Surprisingly, *Muc2*^{+/+} but not *Muc2*^{-/-} became highly susceptible to DSS-induced colitis and lost 10%–15% body weight as early as day 4, and by day 6, mortality rate reached 100% (Figure 2D). In contrast, antibiotic-treated *Muc2*^{-/-} lost 10% body weight between days 7 and 9 (Figure 2E) with negligible mortality. Paradoxically, in mice lacking a mucus barrier alteration of microbiota was refractory against colonic injury. We hypothesized that low-grade inflammation in *Muc2*^{-/-} littermates was inducing a state of immune tolerance in the colon that limited severe injury. Interleukin (IL)-22 cytokine produced by intestinal innate lymphoid cells (ILCs) is implicated to induce immuno-tolerance in the gut²⁸ and might be involved in conferring a protective role to *Muc2*^{-/-} littermates. To test this hypothesis, we isolated colonic LPLs from *Muc2*^{+/+} and *Muc2*^{-/-} and determined IL-22 production by ILCs using flow cytometry. Basally, *Muc2*^{-/-} had higher populations of ILC3 positive for IL-22 as compared with *Muc2*^{+/+} littermates (Figure 2F). Moreover, antibiotics treatment increased IL-22⁺ ILC3 populations in *Muc2*^{-/-} but not in *Muc2*^{+/+} littermates (Figure 2F). The significant increase of IL-22⁺ ILC3 population in antibiotic-treated *Muc2*^{-/-} animals could explain why these mice had higher survival following DSS-induced colitis.

Figure 1. (See previous page). *Muc2*^{-/-} microbiota drives colonic inflammation and increases gut permeability that is normalized following antibiotic treatment. (A) The 16s rRNA sequencing of *Muc2*^{-/-} and *Muc2*^{+/+} littermates stool microbiota before and after antibiotics treatment. Bacterial phyla abundance of untreated *Muc2*^{+/+} (lane a) and *Muc2*^{-/-} (lane b) were similar, with a predominance of Bacteroidetes and Firmicutes. Antibiotics disrupted bacterial population (lanes b and d). (B) Alpha diversity showed equivalent species richness between *Muc2*^{+/+} and *Muc2*^{-/-} littermates, (C) while a difference in beta diversity between the 2 untreated genotypes was evident. Colonic tissues samples from *Muc2*^{-/-} and *Muc2*^{+/+} littermates were analyzed by quantitative polymerase chain reaction for a comparison of proinflammatory cytokines and tight-junction protein expression before and after antibiotics. (D) *Muc2*^{-/-} showed ongoing low-grade inflammation with significantly higher *Tnf-α* and *Il-1β* as compared with untreated *Muc2*^{+/+} littermates. Antibiotics significantly decreased proinflammatory cytokines in *Muc2*^{-/-}. (E) Antibiotic-treated *Muc2*^{-/-} showed reduced constitutive intestinal permeability as measured by FITC dextran, with a correspondent increase in (F) the tight junction proteins occludin and claudin 2. (G) Representative images of fluorescence in situ hybridization using the universal bacterial EUB338–Quasar 670 probe in mouse colonic tissue showing bacteria localization in the lumen. *Ulex europaeus* agglutinin lectin-FITC conjugated was used to visualize mucus. The section was counterstained with DAPI. In *Muc2*^{+/+} bacteria (in red) is present within the mucus layer (green), whereas in *Muc2*^{-/-}, the absence of the mucus layer allowed bacteria to come in contact with the epithelium (white arrows). Scale bar = 50 μm. (H) Comparison of colonic lamina propria CD3⁺ T cells and CD19⁺ B cells at basal level. *Muc2*^{-/-} presented with higher basal levels of T cells and lower levels of B cells in the lamina propria as compared with *Muc2*^{+/+} littermates. (I) Lamina propria lymphocytes from *Muc2*^{+/+} and *Muc2*^{-/-} littermates were isolated and gated through FSC-A vs SSC-A and further interrogated by the ratios of height and width in forward and side scatter to select only single cells population. Thereafter, only live cells were selected using 7-AAD. Live CD19⁺ B cells and CD3⁺ T cells were selected for further analysis, n = 3–4. n = 4–6, *P < .05, **P < .01. Abx, antibiotics; NMDS, nonmetric dimensional scaling.



Microbiota From $Muc2^{-/-}$ Sensitizes the Colonic Mucosa of $Muc2^{+/+}$ Littermates to DSS-Induced Colitis and Mortality

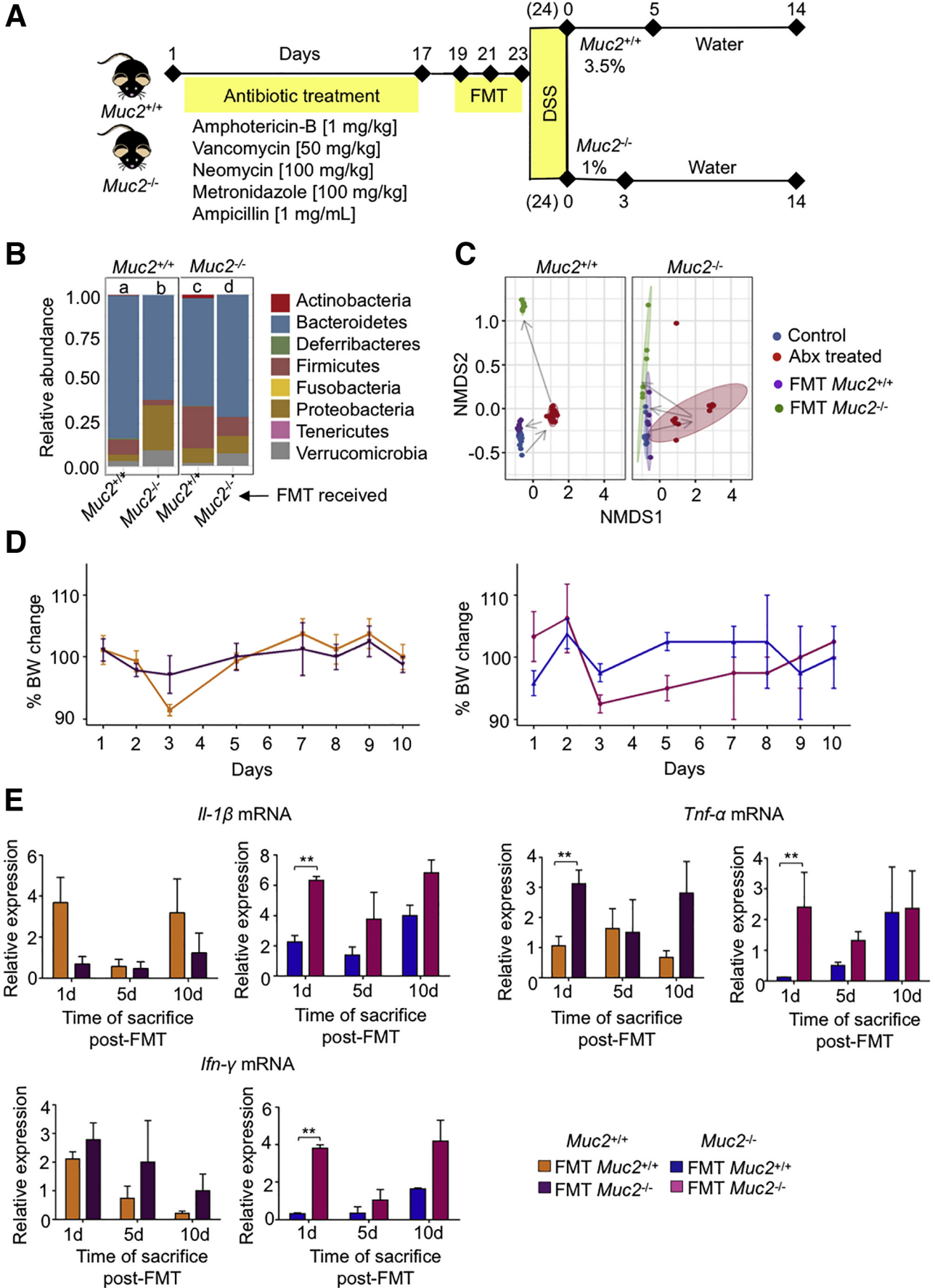
Gut microbiota from ulcerative colitis patients induce inflammation and increase susceptibility to colitis in naive animals.²⁹ To investigate if dysbiotic $Muc2^{-/-}$ microbiota could induce inflammation and/or sensitize $Muc2^{+/+}$ littermates for increase susceptibility to colitis, fecal microbiota transplantation (FMT) was given to antibiotic-treated $Muc2^{+/+}$ and $Muc2^{-/-}$ (homologous and heterologous) using stool from naive age- and sex-matched control animals (see experimental plan in Figure 3A). As revealed by 16s rRNA sequencing, gut bacterial dynamics was restored by FMT in both genotypes (Figure 3B). All FMT groups showed an increase in Bacteroidetes, and Proteobacteria in both genotypes receiving $Muc2^{-/-}$ FMT (Figure 3B). Nonmetric multidimensional scaling plot showed a clear shift in bacterial populations in both genotypes after antibiotic treatment and after receiving FMT (both homologous and heterologous) compared with untreated control animals (Figure 3C). To investigate if $Muc2^{-/-}$ microbiota was proinflammatory, animals were sacrificed on days 1, 5, and 10 after the last FMT and colon samples were analyzed for proinflammatory cytokine messenger RNA (mRNA) levels. Animals showed no significant change in body weight (Figure 3D) up to 10 days regardless of the FMT they received. Similarly, no significant difference in proinflammatory cytokine *Il-1 β* or *Ifn- γ* mRNA levels was observed between groups. $Muc2^{-/-}$ receiving $Muc2^{+/+}$ FMT showed a trend toward less proinflammatory cytokine expression, but the difference was only significant at day 1 (Figure 3E). Similarly, there was a trend in both genotypes receiving $Muc2^{-/-}$ FMT for higher inflammation. These results suggest that $Muc2^{-/-}$ microbiota per se is not colitogenic when transplanted into $Muc2^{+/+}$ littermates.

We next interrogated if FMT altered the susceptibility of the littermates toward DSS colitis. Surprisingly, $Muc2^{+/+}$ receiving $Muc2^{-/-}$ but not $Muc2^{+/+}$ FMT showed significantly higher mortality and impaired restitution at day 14 following DSS-induced colitis (Figure 4A). $Muc2^{+/+}$ receiving $Muc2^{+/+}$ FMT showed little mortality and significantly regained body weights at days 12–14 (Figure 4A). $Muc2^{+/+}$ FMT had no effect on $Muc2^{-/-}$ mortality or body

weight upon DSS challenge (Figure 4B). This was confirmed by improved daily DAI (Figure 4C) and intestinal permeability on day 14 (Figure 4D). In contrast, $Muc2^{+/+}$ receiving $Muc2^{-/-}$ FMT showed significantly higher DAI and increased intestinal permeability (Figures 4C and D).

To investigate the contribution of immune cells and/or gut microbiota as the prime cause for increased sensitivity toward DSS colitis, we generated bone marrow chimeras.³⁰ $Muc2^{-/-}$ receiving bone marrow from $Muc2^{+/+}$ littermates showed similar susceptibility toward DSS induced colitis as compared with $Muc2^{+/+}$ receiving bone marrow from $Muc2^{-/-}$ (Figure 4E). These results confirm that increased susceptibility of $Muc2^{-/-}$ toward DSS is primarily due to the absence of intestinal mucus and has negligible effect on immune cells. In support of this, histopathology showed that compared with untreated $Muc2^{+/+}$ (Figure 5A), and with $Muc2^{+/+}$ receiving their own microbiota (Figures 5B, D, and F), colon samples of $Muc2^{+/+}$ FMT with $Muc2^{-/-}$ microbiota (Figures 5C, E, and G) had significantly higher numbers of ulcerated lesions and damage to crypt architecture. At the height of acute disease on day 7 post-DSS regardless of the FMT, colonic tissues showed thicken muscularis and loss of crypts architecture with similar histological scores (Figures 5B, C, and H). Swiss roll tissue sections of $Muc2^{+/+}$ receiving $Muc2^{-/-}$ microbiota showed marked damage throughout the colon length (Figure 5E), whereas $Muc2^{+/+}$ FMT with their own microbiota presented with less damage in the proximal than the distal colon (Figure 5D). On day 14, $Muc2^{+/+}$ receiving $Muc2^{-/-}$ FMT presented with worst histopathology scores (Figure 5H) characterized by thick muscularis and no signs of crypts regeneration (Figure 5G), whereas $Muc2^{+/+}$ receiving their own FMT showed numerous crypts regenerating with epithelial cell proliferation (Figure 5F). While day 7 histopathology was comparable in $Muc2^{+/+}$ irrespective of the FMT source, at day 14 of disease restitution, $Muc2^{+/+}$ that received $Muc2^{-/-}$ FMT had significantly higher histological scores suggesting impaired recovery in surviving animals (Figure 5H). These results highlight that microbiota from $Muc2^{-/-}$ when transplanted to healthy host ($Muc2^{+/+}$) increases disease susceptibility and impairs tissue healing and recovery following colonic injury.

Figure 2. (See previous page). DSS is lethal to antibiotic-treated $Muc2^{+/+}$ but not $Muc2^{-/-}$ littermates. (A) Sensitivity of $Muc2^{-/-}$ littermates to different dosages of DSS. Animals were treated with different dosages of DSS and weight loss was examined. In all groups, approximately 10%–20% weight loss was observed, but recovery as assessed by weight gain was only evident in animals given 1% for 3 days. Each data point represents the mean \pm SEM per animal group per day. $n = 5$ animals per group. (B) $Muc2^{+/+}$ are resistant to low dose DSS as compared with $Muc2^{-/-}$ littermates. Littermates were treated with 1% DSS (3d) after which DSS was replaced with tap water. DSS induced $\sim 15\%$ weight loss in $Muc2^{-/-}$ between day 6 and day 9 whereas $Muc2^{+/+}$ mice showed no weight loss. Each data point represents the mean \pm SEM per group per day; control animals $n = 3$, $Muc2^{-/-}$ DSS $n = 5$, $Muc2^{+/+}$ DSS $n = 10$. (C) Diagrammatic work plan: briefly, $Muc2^{+/+}$ and $Muc2^{-/-}$ littermates received an antibiotic cocktail for 17 days and 1 day after were given DSS in drinking water. $Muc2^{+/+}$ received 3.5% DSS for 5 days while $Muc2^{-/-}$ received 1% DSS for 3 days, followed by ad libitum water. Mice were sacrificed on day 14 following DSS treatment. Control nonantibiotic-treated mice received the same % of DSS. (D) Antibiotic treated $Muc2^{+/+}$ were highly susceptible to DSS and lost weight faster and reached 100% mortality by day 6 as compared with untreated $Muc2^{+/+}$ subjected to the same DSS regime. (E) In $Muc2^{-/-}$ littermates, no significant changes in DSS susceptibility were observed between animals that received antibiotics or not. (F) Isolated lamina propria cells from $Muc2^{+/+}$ and $Muc2^{-/-}$ littermates were characterized by flow cytometry. $Muc2^{-/-}$ ILC3 population was significantly increased after antibiotic treatment. IL-22 antibody was used to characterize ILC3 cell population. $n = 4$ –6, * $P < .05$. BW, body weight.



Presence of Tolerogenic Immune Cells in Colonic Lamina Propria of *Muc2*^{-/-} Littermates

Given that *Muc2*^{-/-} has low-grade ongoing inflammation and its microbiota increases disease susceptibility to *Muc2*^{+/+} littermates, we next explored the mechanisms through which *Muc2*^{-/-} tolerate their microbiota to cope with basal inflammation. A recent study³¹ suggested that *Muc2*^{-/-} develop spontaneous colitis due to a reduction in CD103⁺CD11b⁻ and an increase in CD103⁺CD11b⁺ dendritic cells (DCs) population. Based on this, we characterized the immune cell populations. Under basal conditions, *Muc2*^{-/-} littermates presented with significantly higher levels of CD45⁺MHCII⁺ cell populations (Figures 6A and B). Cells were gated based on CD11b and CD11c expression (Figures 6A and C). These cells are predominantly phagocytes that help clear incoming microbial penetrants at the colonic surface. We also observed increased levels of colonic CD103⁺CD11c⁺ (R1) DCs population in *Muc2*^{-/-} littermates (Figures 6C–E), which may potentiate the development and proliferation of T regulatory cells (Tregs). In support of this, we quantified CD4⁺FoxP3⁺ cells in small intestine and colonic LPLs and observed that basally, *Muc2*^{-/-} exhibited higher populations of CD4⁺FoxP3⁺ Tregs as compared with *Muc2*^{+/+} (Figure 6F). To confirm a role for Tregs in maintaining the *Muc2*^{-/-} inflammatory phenotype in-check, we neutralized Tregs effector molecules IL-10 and transforming growth factor β (TGF- β), which have potent anti-inflammatory effects. *Muc2*^{-/-} mice lost weight rapidly after injection of anti-IL-10 and anti-TGF- β antibodies and by day 5 post-injection, their weight loss was significantly lower compared with *Muc2*^{+/+} (Figure 6G). Five days after injection, *Muc2*^{+/+} treated and control animals showed no visual differences whereas, treated *Muc2*^{-/-} mice presented with watery stool consistency and shorter and thicker colons (Figure 6H). This was accompanied with higher mRNA expression for proinflammatory cytokines *Il-1 β* and *Ifn- γ* (Figure 6I) as well as myeloperoxidase activity (Figure 6J) as compared with untreated control animals. These results clearly show that the intestinal microbiota in *Muc2*^{-/-} littermates induces the recruitment of tolerogenic immune cells at colonic sites that allow them to mitigate the damage caused by an inflammatory phenotype.

The Impact of *Muc2*^{-/-} Microbiota Could Be Explained Through Operational Taxonomic Units From Distinctive Families That Are Transplantable to *Muc2*^{+/+} Littermates

To determine if the biologic effects seen with *Muc2*^{-/-} microbiota over *Muc2*^{+/+} littermates was associated with a

putative bacteria group, we performed 16s rDNA-sequencing analysis on day -17 (before antibiotics) and on days 1, 5, and 10 after receiving antibiotics and all 3 FMT (Figures 7A–G). On day 1, both *Muc2*^{+/+} and *Muc2*^{-/-} FMT with their own microbiota (Figure 6A, blue circles in panels b and c) displayed a bacterial composition similar to their preantibiotics state (red circles). However, at this same time point (day 1), a difference in composition was noticeable in *Muc2*^{-/-} receiving *Muc2*^{+/+} FMT (Figure 7A, panel a) and specially contrasting in *Muc2*^{+/+} receiving *Muc2*^{-/-} FMT (Figure 7A, panel d) that corresponded with a significant drop in alpha diversity in *Muc2*^{+/+} at day 1 after receiving *Muc2*^{-/-} FMT (Figure 8A). When compared with their preantibiotics state, these differences are not maintained throughout time since the diversity returns to a more similar preantibiotic state as soon as 5 days after the last FMT and alpha diversity was similar among treatments (Figure 7A). Based on these results, we next compared microbiota composition between both FMT in *Muc2*^{+/+} (FMT with *Muc2*^{-/-} vs FMT with homologous) at day 1. Results revealed differences in bacterial composition with those receiving *Muc2*^{-/-} FMT having up to 6 times more operational taxonomic units (OTUs) from Enterobacteriaceae and higher amounts of the Verrucomicrobiaceae family (Figure 8B). In contrast, there was a decrease in OTUs from some Proteobacteria families such as Pseudomonadaceae and Desulfovibrionaceae. OTUs from the Anaeroplasmataceae and Deferribacteraceae families were also decreased, along with some Firmicutes families such as Ruminococcaceae, Lactobacillaceae, Lachnospiraceae, and Bacillaceae and some Bacteroidetes families like Prevotellaceae, Rikenellaceae, and particularly S24-7 experienced a decrease in their populations when compared with the ones FMT with *Muc2*^{+/+} microbiota (Figure 8B).

OTUs among both FMT in *Muc2*^{+/+} were grouped by family, and the 5 most abundant were plotted to contrast their abundance per FMT treatment and time points (Figure 7B), these being Bacteroidaceae, Lactobacillaceae, S24-7, Enterobacteriaceae, and Verrucomicrobiaceae families. At day 1 post-FMT, a dramatic difference between both FMT treatments was observed, where *Muc2*^{+/+} FMT with *Muc2*^{-/-} showed increase abundance in members of the Bacteroidaceae family (Figures 7B and C), as well as members of the Enterobacteriaceae family (Figures 7B and F) and Verrucomicrobiaceae (Figures 7B and G). In contrast, members of the Lactobacillaceae (Figures 7B and D) and the

Figure 3. (See previous page). C57BL/6 and in-house *Muc2*^{-/-} have different bacteria phyla distribution. (A) Diagrammatic work plan. Briefly, *Muc2*^{+/+} and *Muc2*^{-/-} antibiotic-treated mice received FMT every other day before giving DSS in drinking water. *Muc2*^{+/+} received 3.5% DSS for 5 days while *Muc2*^{-/-} received 1% DSS for 3 days, followed by ad libitum water. Mice were sacrificed on day 14 following DSS treatment. (B) The 16s rRNA sequencing comparison of bacterial phyla abundance in *Muc2*^{+/+} and *Muc2*^{-/-} littermates receiving either homologous or opposite genotype FMT. Analysis shows the results of day 1 post-FMT. (C) Nonmetric multidimensional scaling (NMDS) analysis of samples was performed to plot population distribution between each sample, in which a clear separation between groups is seen. (D) *Muc2*^{-/-} and *Muc2*^{+/+} mice were treated for 17 days with an antibiotic cocktail and received FMT with either *Muc2*^{-/-} or *Muc2*^{+/+}. Animals were sacrificed 1, 5, and 10 days after FMT. No significant differences in weight change were observed between the 4 groups. (E) *Muc2*^{+/+} receiving *Muc2*^{-/-} FMT showed no significant increase in proinflammatory cytokines compared with control animals receiving their own FMT. Relative expression as compared with its own untreated control animal. n = 3–4, *P < .05, **P < .01. Abx, antibiotics; BW, body weight.

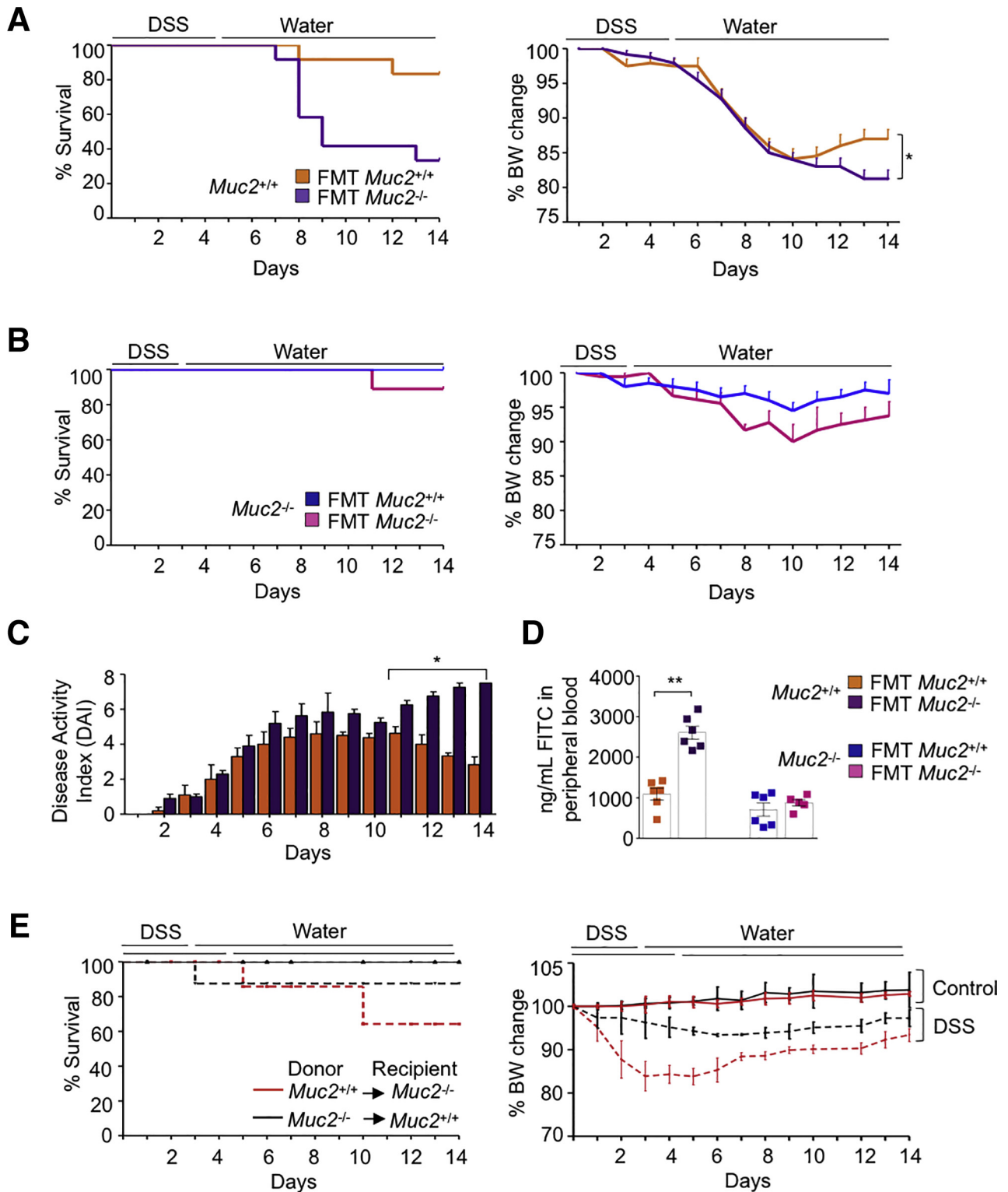
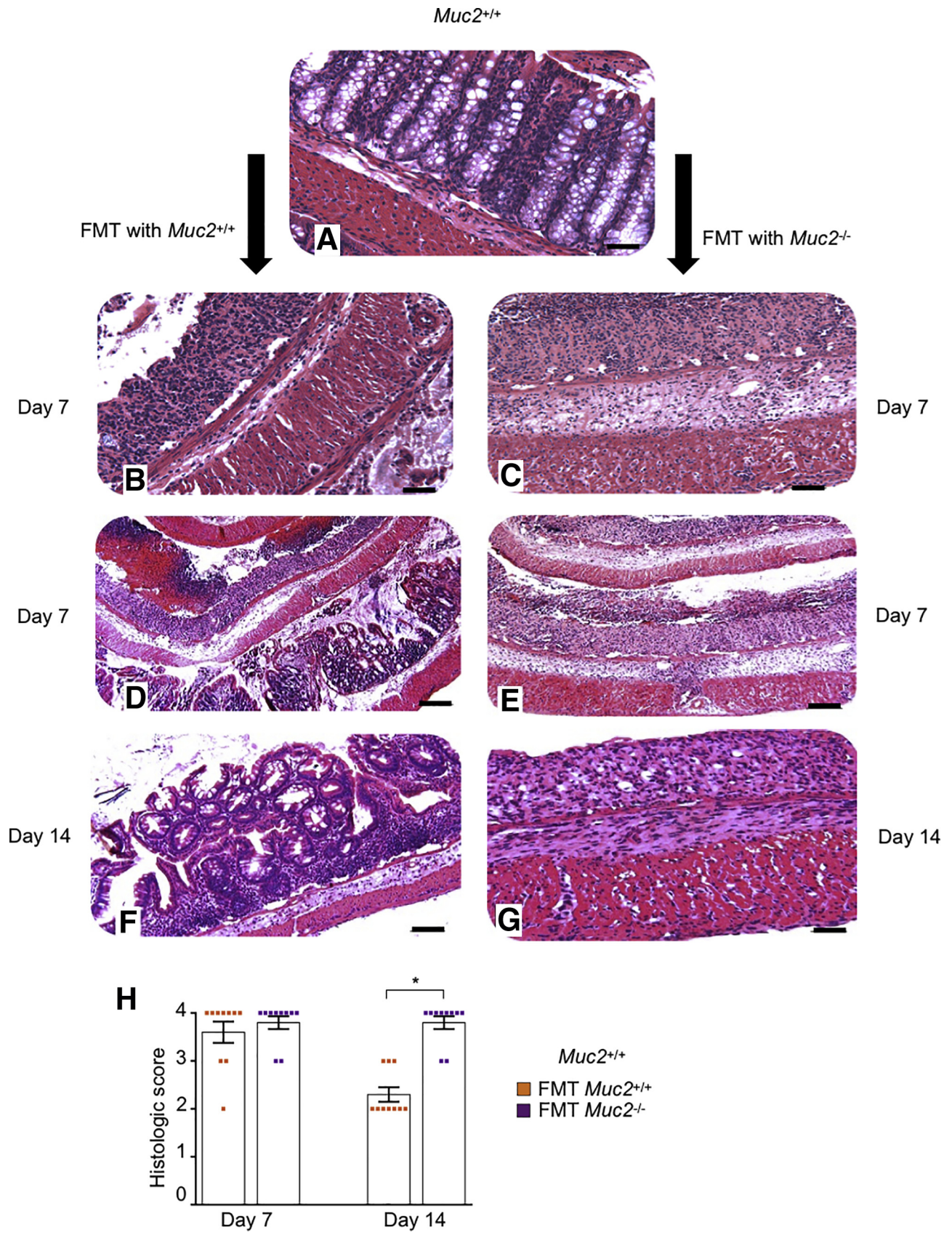


Figure 4. $Muc2^{-/-}$ FMT increases susceptibility to DSS-induced colitis in $Muc2^{+/+}$ littermates. (A) Antibiotic treated $Muc2^{+/+}$ receiving $Muc2^{-/-}$ FMT showed increased mortality to DSS induced colitis and the surviving animals did not recover weight up to day 14. (B) $Muc2^{-/-}$ mice receiving $Muc2^{+/+}$ FMT showed less severe illness and no mortality in response to DSS induced colitis. (C) $Muc2^{+/+}$ mice receiving $Muc2^{-/-}$ FMT showed an increased in DAI compared with those who received their own. (D) On day 14, $Muc2^{+/+}$ receiving $Muc2^{-/-}$ FMT showed increased intestinal permeability as compared with $Muc2^{+/+}$ receiving their own microbiota. (E) Survival and body weight change of $Muc2^{+/+}$ and $Muc2^{-/-}$ bone marrow (BM) chimeras challenged with DSS. $n = 4-6$, * $P < .05$, ** $P < .01$, BW, body weight.



S24-7 family were reduced in these mice (Figures 7B and E). *Muc2*^{-/-} FMT with their own microbiota also showed an increase in the Bacteroidaceae (Figure 7C), Enterobacteriaceae (Figures 7F), and Verrucomicrobiaceae (Figure 7G) families. It is noteworthy that these changes in bacterial dynamics are not permanent, because 10 days after the last FMT the differential abundance came back to their normal state. These results give strong evidence that these bacteria played a primordial role in mucosal sensitization to DSS when *Muc2*^{+/+} received *Muc2*^{-/-} FMT.

We also used phylogenetic investigation of communities by reconstruction of unobserved states (PICRUST)³² to predict metabolic differences and to identify their potentially distinctive functional features among the samples. Metagenomes were predicted from the 16S rRNA data and differences were focused in *Muc2*^{+/+} receiving either *Muc2*^{-/-} or their own FMT (Figure 9). Among them, important pathways related with gram-negative pathogens are proposed to be up regulated in those receiving *Muc2*^{-/-} FMT, such as genes involved in biofilm of *E. coli*, *Pseudomonas aeruginosa*, and *Vibrio cholerae*, as well as genes related to lipopolysaccharide biosynthesis, flagellar assembly, and glutathione metabolism (Table 1). Genes that were downregulated in *Muc2*^{+/+} receiving *Muc2*^{-/-} FMT included some involved in methane, carbon, and butyrate metabolism. Therefore, we were interested in exploring the contributions of taxa to each of the predicted pathways across the sample groups. Several families within different phylum were related to those predicted changes in the metagenome. Bacteroidetes family S24-7 was represented in high proportion among all pathways, both up- and downregulated and at different time points and FMT treatments. Likewise, the Bacteroidaceae family was also present among up- and downregulated pathways throughout all the samples but is less represented than S24-7. Interestingly the family Enterobacteriaceae was also present in both up- and downregulated pathways, but with a noticeable increase to the pathway contribution at day 1 after FMT with *Muc2*^{-/-} microbiota (Figure 9, Table 1).

Discussion

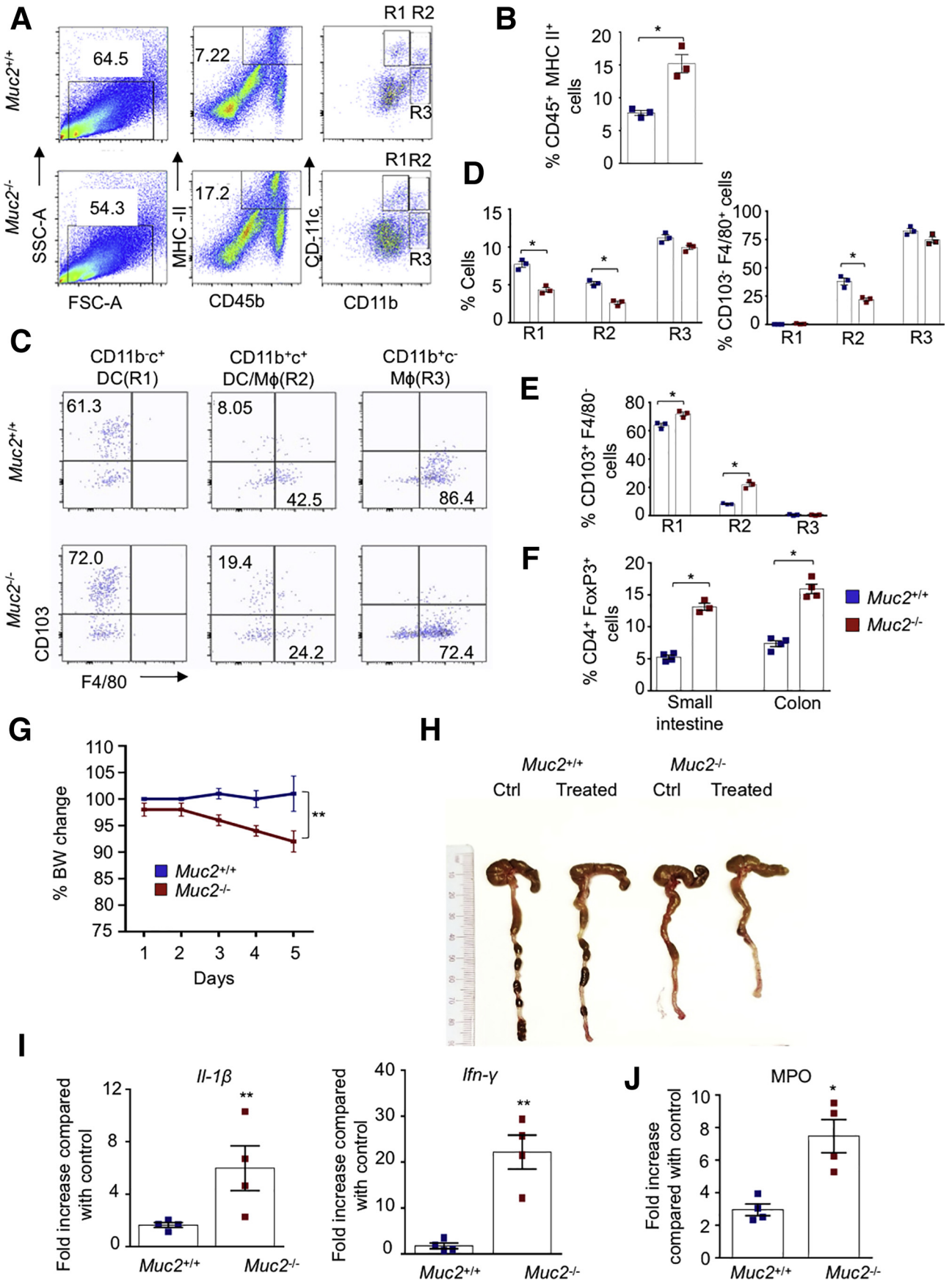
Gut microbiota is essential to human health and mucus provides them with a niche and food source to thrive.^{13,16} Dysbiosis and depletion of mucus have been implicated with colonic inflammation and IBD.^{33,34} Thus,

understanding the distinct roles of the microbiota in the presence or absence of the mucus bilayer in innate host defense is critical in understanding disease pathogenesis. In this study we have revealed shifts in microbial populations in the absence of a mucus layer. These bacteria were found in direct contact with the epithelium that elicited low-grade inflammation that was counteracted with an increase in immune tolerogenic cells. In turn, this microbiota when transplanted into WT littermates sensitized their mucosa for increased intestinal injury.

The role of mucus layer in development and regulation of the immune system is increasingly recognized as it separates gut bacteria from intestinal immune cells.³⁵ In IBD, commensal bacteria are the target of host immune aggression, thus triggering an inflammatory phenomena and perpetuating mucosal destruction.³⁶ Our study shows that close contact of bacteria with the intestinal epithelium creates a proinflammatory milieu evidenced by increased levels of *Tnf-α* and *Il-1β* that in turn potentiated intestinal permeability. Surprisingly, however, was that antibiotic-treated *Muc2*^{-/-} showed no severity to DSS-induced mortality whereas *Muc2*^{+/+} littermates succumb to the injury emphasizing the protective role of gut microbiota for proper functioning of immune system. IL-22 cytokine, mainly released by ILC3, plays a key role in maintaining gut-microbial homeostasis, epithelial barrier function and stimulating tissue repair in the colon.^{37,38} The ILC3-IL22 axis has also been found to be important in regulating immune response against extracellular pathogens (bacteria and fungus), as well as preventing their translocation through the stimulation of antimicrobial peptides, reviewed in Geremia and Arancibia-Cárcamo.³⁹ A link between IL-22 and *Muc2* has been suggested^{28,40}; however, the exact mechanism and how it is regulated it is not yet fully understood. Higher levels of IL-22 have been reported in the ileum of *Muc2*^{-/-} mice.²⁸ We theorize that high levels of ILC3-IL-22 in *Muc2*^{-/-} littermates induced a tolerance state that allowed them to cope with ongoing mild inflammation without developing fulminant colitis.

Mucosal tolerance is critical in maintaining intestinal homeostasis, and to provide an immune exclusion state against commensal microbiota.^{41,42} This is mainly maintained by lamina propria DCs as they sample the microbial content and stimulate Tregs to produce anti-inflammatory IL-10 and TGF-β.^{43,44} We observed the presence of higher number of CD45⁺MHCII⁺ phagocytic cells in the lamina

Figure 5. (See previous page). *Muc2*^{+/+} receiving *Muc2*^{-/-} FMT impaired tissue healing and crypts regeneration following DSS-induced colitis. (A) Representative images of hematoxylin and eosin-stained Swiss-rolled colons from untreated control showing normal architecture with crypts filled with goblet cells. (B, D, and F) *Muc2*^{+/+} receiving *Muc2*^{+/+} FMT and (C, E, and G) *Muc2*^{+/+} receiving *Muc2*^{-/-} FMT. Note loss of crypts architecture, ulcerated lesions and thickness of the muscularis in both (B) *Muc2*^{+/+} receiving *Muc2*^{+/+} FMT and (C) *Muc2*^{+/+} receiving *Muc2*^{-/-} FMT microbiota at day 7. (D) Swiss roll sections showed that *Muc2*^{+/+} receiving *Muc2*^{+/+} FMT lesions were restricted to the mid and distal colon. (E) *Muc2*^{+/+} receiving *Muc2*^{-/-} FMT showed more intense tissue damage with complete loss of crypts and damage throughout the length of the colon. (F) In contrast, at disease resolution on day 14, *Muc2*^{+/+} receiving *Muc2*^{+/+} FMT showed crypts restitution and epithelial cell proliferation with a normal muscularis, (G) while no crypts regeneration and a thick muscularis were predominant in *Muc2*^{+/+} receiving *Muc2*^{-/-} FMT. Scale bar = 50 μm in A, B, C, F, and G. Scale bar = 200 μm in D and E. (H) Blinded histologic score values at days 7 and 14 post-DSS. At day 7, the histologic score was comparable between both groups, however, at disease recovery phase on day 14, *Muc2*^{+/+} receiving *Muc2*^{-/-} FMT had significantly higher histologic scores than the group that received homologous FMT. n = 10, *P < .05.



propria of *Muc2*^{-/-} than in *Muc2*^{+/+} littermates. This, no doubt exerted a protective effect as *Muc2*^{-/-} had higher gut microbial penetrants in the absence of a mucus barrier. Similarly, we also found increased populations of colonic CD103⁺CD11c⁺ DCs in *Muc2*^{-/-}, critical for establishing tolerance and to withstand ongoing low-grade colonic inflammation.³¹ Because differences in microbial dynamics present in untreated animals would not reflect the bacteria that are transplantable, we identified differences between both FMT groups (homologous and heterologous) in *Muc2*^{+/+} littermates. We found that the Bacteroidaceae family was significantly increased in both genotypes receiving *Muc2*^{-/-} microbiota, particularly in *Muc2*^{+/+} recipients (4-fold increase). Bacteroides is a clinically relevant group of bacteria and includes many known pathogens having unique secretion systems, endotoxins and virulence factor genes that provides them antimicrobial resistance.^{45,46} A recent study using *Muc2*^{-/-} mice, linked the genus Bacteroides to susceptibility toward DSS-induced colitis and altered gene expressions associated with bacteria sensing and stress response.⁴⁷ OTUs from the family Verrucomicrobiaceae were significantly increased within both genotypes receiving *Muc2*^{-/-} FMT. This family is of special interest as it includes the mucin degrading bacteria *Akkermansia muciniphila*, a commensal associated with maintaining homeostasis. Their reduced levels have been reported in patients with IBD and various metabolic disorders.⁴⁸ We also noticed a reduction in OTUs of Lactobacillaceae family, which are lactic acid-producing bacteria and considered as important probiotics for their positive effects on host health.^{49,50} Recently,⁵¹ it was established that within the first 3 weeks of colonization, the gut bacterial population goes through a series of changes until becoming stable, making evident the dynamics of microbiota population after being transferred to a new host.

PICRUSt is a valuable bioinformatics tool that allows to make predictions of genes and/or metabolic pathways that might be over or under-expressed.³² Table 1 summarizes the predicted metabolic pathways that were significantly different between microbiota within *Muc2*^{+/+} receiving either *Muc2*^{-/-} or homologous FMT. We observed upregulated pathways that were related to gram-negative pathogens, such as genes involved in biofilm formation of

V. cholerae, *E. coli*, and *P. aeruginosa*. Biofilm formation plays an important role in bacterial infections, sheltering them from the host immune defense and allowing them to attach, proliferate and spread inside of the host.⁵² Similarly, we observed upregulation of genes involved in glutathione metabolism. Within bacteria, glutathione is only present in Cyanobacteria and Proteobacteria and is used as a protecting mechanism in different stress triggers such as low pH and oxidative stress. In addition, up regulation of genes involved in lipopolysaccharide biosynthesis were also predicted. The up regulation of these pathways correlates and could be explained due to a higher relative abundance of gram-negative Proteobacteria, particularly family Enterobacteriaceae in *Muc2*^{+/+} receiving *Muc2*^{-/-} FMT.

In summary, we have identified a distinctive gut microbiota in *Muc2*^{-/-} littermates in the absence of mucus that maintains a constitutive proinflammatory milieu in their colon. This unique microbial population did not trigger basal proinflammatory responses when transplanted into *Muc2*^{+/+} littermates but rather, sensitized the colonic mucosa for increased sensitivity toward DSS-induced colitis. Unlike *Muc2*^{-/-}, *Muc2*^{+/+} microbiota played a protective role against chemical-induced colitis that was lost following antibiotic treatment. A limitation of the study is that despite the phenotypic effects of the different treatments being comparable in *Muc2*^{-/-} vs *Muc2*^{+/+}, it is difficult to ascertain the difference in immune response and microbiota changes as those effects may be independent of the level of inflammation induced and could be a direct effect of the drug itself. We conclude that both the colonic mucus layer and indigenous microbiota play key roles in conferring innate resistance against colonic injury and homeostasis.

Materials and Methods

Ethics Statement and Animals

Eight- to 12-week-old male and female C57BL/6 and *Muc2*^{-/-} mice were used. C57BL/6 mice were obtained from Charles River Laboratories (Saint-Constant, Quebec, Canada), while *Muc2*^{-/-} of the same genetic background was bred in house. Animals were backcrossed to generate *Muc2*^{+/-} breeding pairs to derive *Muc2*^{+/+} and *Muc2*^{-/-} littermates that were used for the experiments. All animals were housed under specific pathogen-free conditions in

Figure 6. (See previous page). **Characterization of immune cells in the colonic lamina propria of *Muc2*^{+/+} and *Muc2*^{-/-} littermates.** Lamina propria cells were isolated and stained with antibodies for DCs/Mφ and a viability dye (7-AAD). (A) Gating strategy for characterization of different population of DCs and macrophages in lamina propria of *Muc2*^{+/+} and *Muc2*^{-/-} littermates. Fluorescence-activated cell sorter plot displaying live cells gated on MHCII and CD45 and then analyzed for CD11b⁺ and CD11c⁺ cells. (B) Cumulative data showing percentage populations of live CD45⁺ MHCII⁺ cells in lamina propria of *Muc2*^{+/+} and *Muc2*^{-/-} littermates. (C) Different regions of cells (R1, R2, and R3) expressing various levels of CD11b and CD11c were further gated for CD103 and F4/80. (D) Cumulative data showing percentage populations of DCs/Mφ cells among CD45⁺ MHCII⁺ cells on the basis of CD11b and CD11c expression in lamina propria of *Muc2*^{-/-} littermates (R1 = MHCII⁺CD45⁺CD11c⁺CD11b⁻; R2 = MHCII⁺CD45⁺CD11c⁺CD11b⁺; and R3 = MHCII⁺CD45⁺CD11c⁺CD11b⁺). (E) Cumulative data showing expression levels of CD103 and F4/80 among R1, R2, and R3 populations. (F) Increased population of CD4⁺FoxP3⁺ T-regs at basal level in small intestine and colonic lamina propria of *Muc2*^{-/-} compared with *Muc2*^{+/+} littermates. (G) Anti-IL-10 and anti-TGFβ antibodies were injected intraperitoneally into *Muc2*^{+/+} and *Muc2*^{-/-} littermates and percentage of body weight change measured up to 5 days. (H) Representative image of mice colon and cecum 5 days post anti-IL-10 and anti-TGF-β injection. (I) mRNA expression of proinflammatory cytokines IL-1β and interferon gamma (IFN-γ) in animals treated with antibodies, compared with respective untreated control animals. (J) Myeloperoxidase (MPO) activity in colon of mice 5 days post-antibodies injection. n = 3–4, *P < .05, **P < .01.

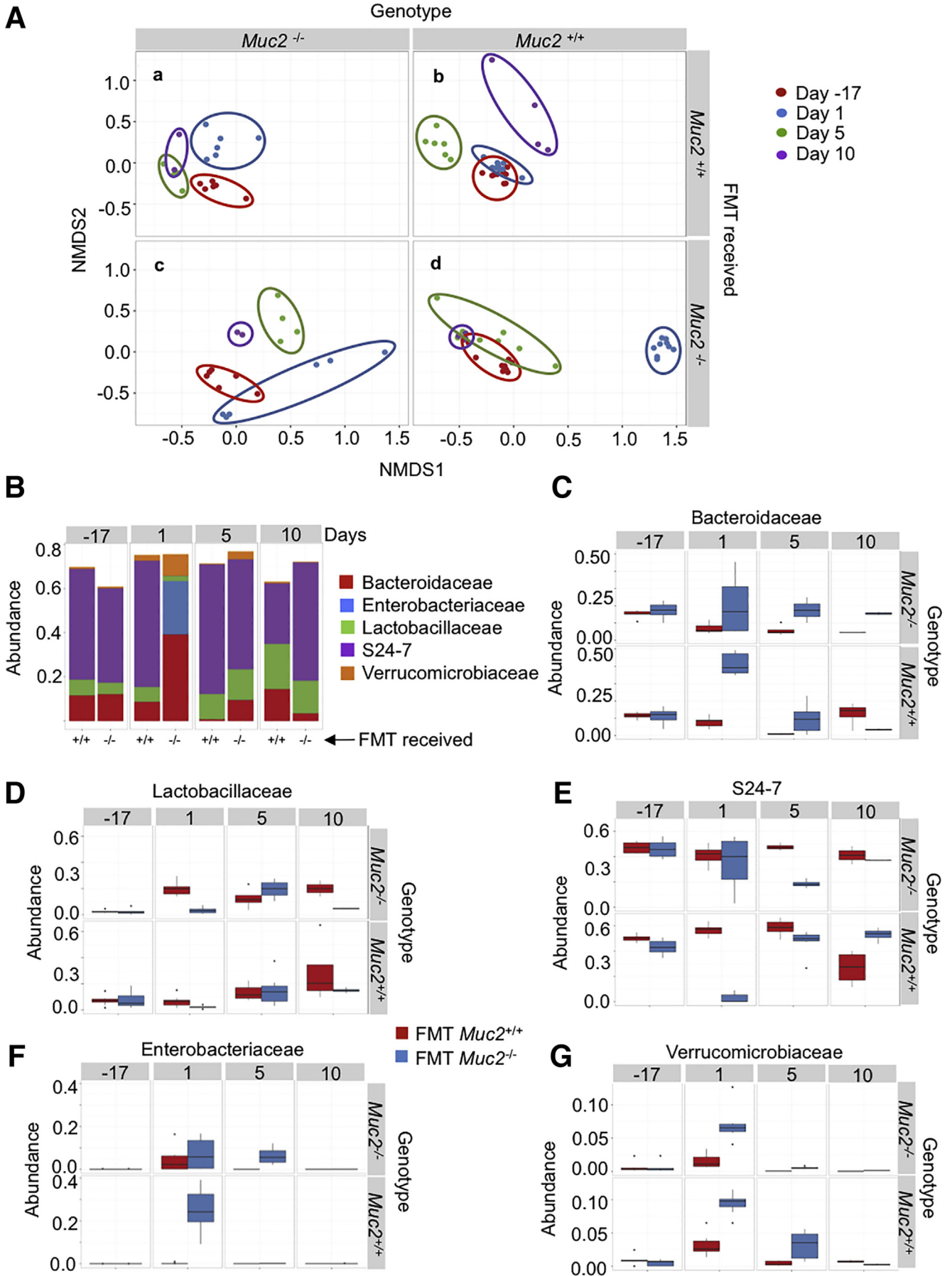


Table 1. PICRUSt Prediction of Significantly Different Metabolic Pathways Between *Muc2*^{+/+} FMT With *Muc2*^{-/-} or Homologous Microbiota

Pathway	KEGG ID	<i>P</i> value	Adjusted <i>P</i> value	Normalized enrichment score
Biofilm formation - <i>Vibrio cholerae</i>	map05111	2.5×10^{-5}	.0014	2.2
Biofilm formation - <i>Escherichia coli</i>	map02026	2.6×10^{-5}	.0014	2.1
<i>Staphylococcus aureus</i> infection	map05150	7.1×10^{-5}	.0017	-2.6
Aminoacyl-tRNA biosynthesis	map00970	7.9×10^{-5}	.0017	-2.2
Lipopolysaccharide biosynthesis	map00540	8×10^{-5}	.0017	1.9
Ribosome	map03010	9.9×10^{-5}	.0018	-2.7
Methane metabolism	map00680	.00012	.0018	-2.7
Carbon metabolism	map01200	.00029	.0039	-1.8
Biosynthesis of siderophore group nonribosomal peptides	map01053	.00088	.0099	1.8
Flagellar assembly	map02040	.00092	.0099	1.8
Carbon fixation pathways in prokaryotes	map00720	.0035	.032	-1.6
Cationic antimicrobial peptide (CAMP) resistance	map01503	.0041	.034	1.7
Glutathione metabolism	map00480	.0052	.038	1.7
Biofilm formation - <i>Pseudomonas aeruginosa</i>	map02025	.0052	.038	1.6
Butanoate metabolism	map00650	.0061	.041	-1.5

FMT, fecal microbiota transplantation; KEGG, Kyoto Encyclopedia of Genes and Genomes; PICRUSt, phylogenetic investigation of communities by reconstruction of unobserved states;

filter-top cages and fed autoclaved food and water ad libitum. Throughout the study, animals were closely monitored to ensure healthy conditions and all experiments adhered to the University of Calgary Animal Care Committee standards.

Antibiotic Treatment

Muc2^{+/+} and *Muc2*^{-/-} littermates were treated with antibiotics to decrease bacterial load as described previously.²³ In brief, mice were gavaged every 12 hours with an antibiotic cocktail as follows: for the first 3 days, mice were gavaged with amphotericin-B (1 mg/kg) to suppress fungal growth. From day 4, ampicillin (1 mg/mL) was added to the drinking water; in addition, mice received orally vancomycin (50 mg/kg), neomycin (100 mg/kg), metronidazole (100 mg/kg), and amphotericin-B (1 mg/kg) for another 14 days. This combination ensured the safe and controlled delivery of antibiotics to each mouse while having a broad-spectrum effect.

Fecal Microbiota Transplantation

FMT was achieved by collecting 0.1g of fresh feces (about 4 fecal pellets), homogenizing in 1 mL of sterile phosphate-buffered saline and centrifuged for 30 seconds at 1000 *g*. Each mouse was gavaged 3 times with 200 μ L of the obtained supernatant every 48 hours.

DSS-Induced Colitis

Colitis was induced using DSS (MW: 36,000–50,000; MP Biochemicals, Santa Ana, CA) dissolved in tap water. *Muc2*^{-/-} animals received 1% for 3 days, while *Muc2*^{+/+} mice received 3.5% for 5 days follow up by water ad libitum as previously described.¹⁷ The cumulative DAI was scored based on weight loss, stool consistency, blood loss, and appearance as previously described.²⁰

OTU Table Construction

Raw reads were processed with cutadapt 1.8.3⁵³ to remove the primer sequences and any preceding adaptors. Subsequent processing was done using the UPARSE pipeline⁵⁴ as implemented in usearch 8.1.1861. The forward and reverse reads were merged using the fastq_mergepairs option of usearch and subsequently filtered with usearch -fastq_filter and an expected error cutoff of 0.5.⁵⁵ The filtered reads were de-replicated using usearch -derep_fulllength and then clustered with usearch -cluster_otus and the option '-minsize 2' to remove singleton reads prior to clustering. Taxonomy was assigned to the representative sequences using the RDP-naïve Bayesian classifier⁵⁶ with May 2013 version of the Greengenes database. The final OTU table was constructed with usearch -usearch_global and the options '-strand plus -id 0.97'. The entire procedure was run as a Snakemake pipeline.⁵⁷

Figure 7. (See previous page). *Muc2*^{-/-} microbiota transplanted to *Muc2*^{+/+} littermates. (A) Dissimilarity measured by nonmetric multidimensional scaling (NMDS) illustrates the distance throughout samples that were antibiotic-treated and FMT with *Muc2*^{-/-} and *Muc2*^{+/+} microbiota. Time points are as follow: day -17: before antibiotic treatment, days 1, 5, and 10 correspond to days passed after the last FMT; (a) *Muc2*^{-/-} FMT with *Muc2*^{+/+}, (b) *Muc2*^{+/+} FMT with *Muc2*^{+/+}, (c) *Muc2*^{-/-} FMT with *Muc2*^{-/-}, and (d) *Muc2*^{+/+} FMT with *Muc2*^{-/-}. (B) Significantly different OTUs between *Muc2*^{+/+} FMT with *Muc2*^{-/-} and *Muc2*^{+/+} were grouped by family and the top 5 plotted in a bar graph to illustrate their difference in abundance. Plots C–G display the 5 families' dynamics at different time points.

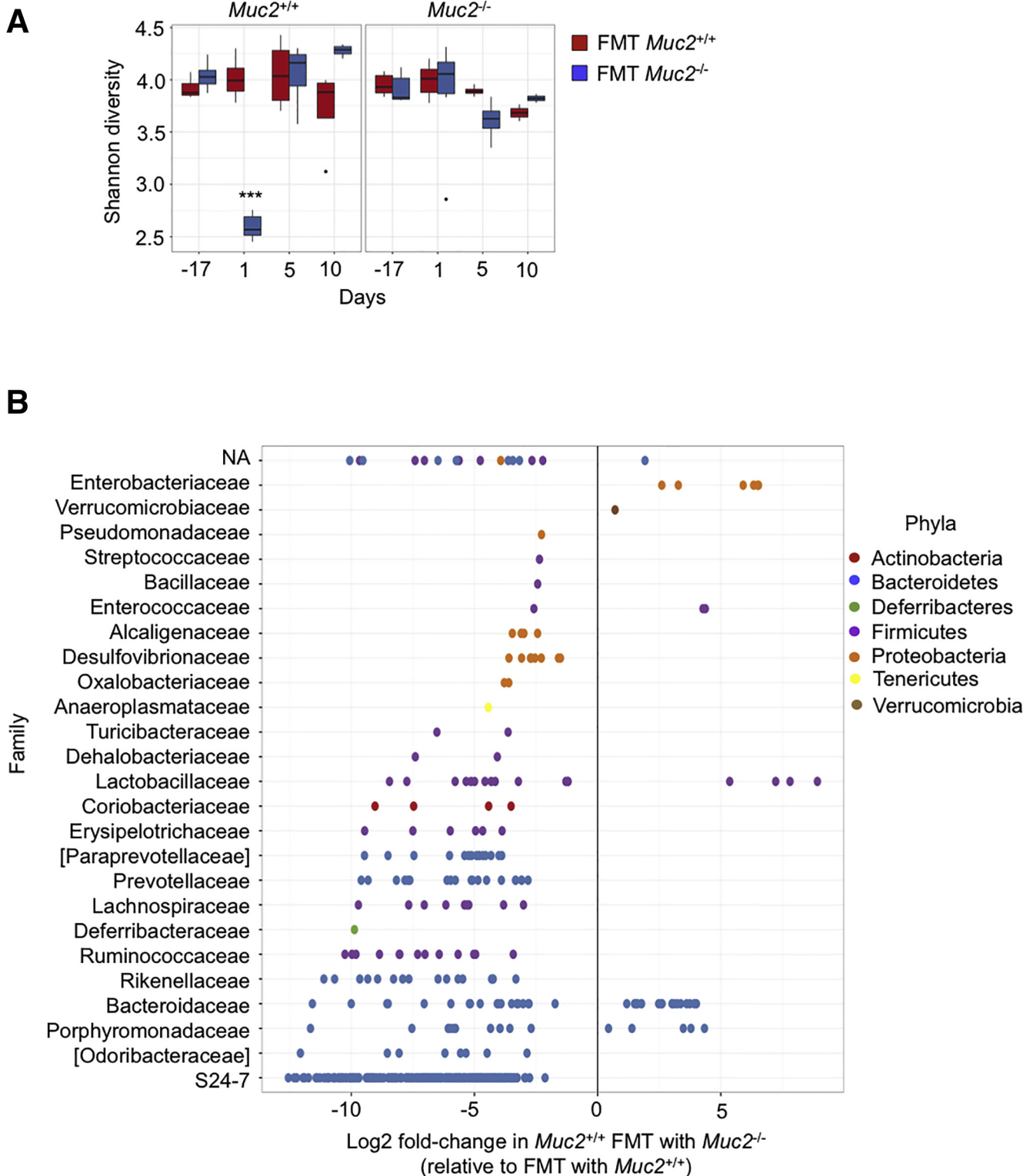


Figure 8. Fecal transplant of *Muc2*^{-/-} into *Muc2*^{+/+} changes bacteria family abundance and decreases their alpha diversity. (A) Alpha diversity of *Muc2*^{+/+} and *Muc2*^{-/-} was characterized by Shannon's index in *Muc2*^{+/+} and *Muc2*^{-/-} littermates at different time points; before antibiotic treatment (day -17), and 1, 5, and 10 days after receiving the last FMT (day, 1, 5, and 10, respectively). Notice the drop in species diversity in the *Muc2*^{+/+} group at day 1 after FMT with *Muc2*^{-/-} microbiota. Wilcoxon rank sum test for differences in Shannon diversity between *Muc2*^{+/+} treatment and *Muc2*^{-/-} treatment. *P* values are adjusted for multiple testing using the Benjamini and Hochberg method. (B) Differential abundance, at the family level, between *Muc2*^{+/+} FMT with *Muc2*^{+/+} and *Muc2*^{-/-} microbiota based on 16S rDNA from *Muc2*^{+/+} FMT with either *Muc2*^{-/-} or their own microbiota. Results are shown as fold-change in *Muc2*^{+/+} FMT with *Muc2*^{-/-} relative to *Muc2*^{+/+} FMT with *Muc2*^{+/+}. Log₂ fold-changes are plotted for significantly different (*P* < .05) family for each of the comparisons. ****P* < .001.

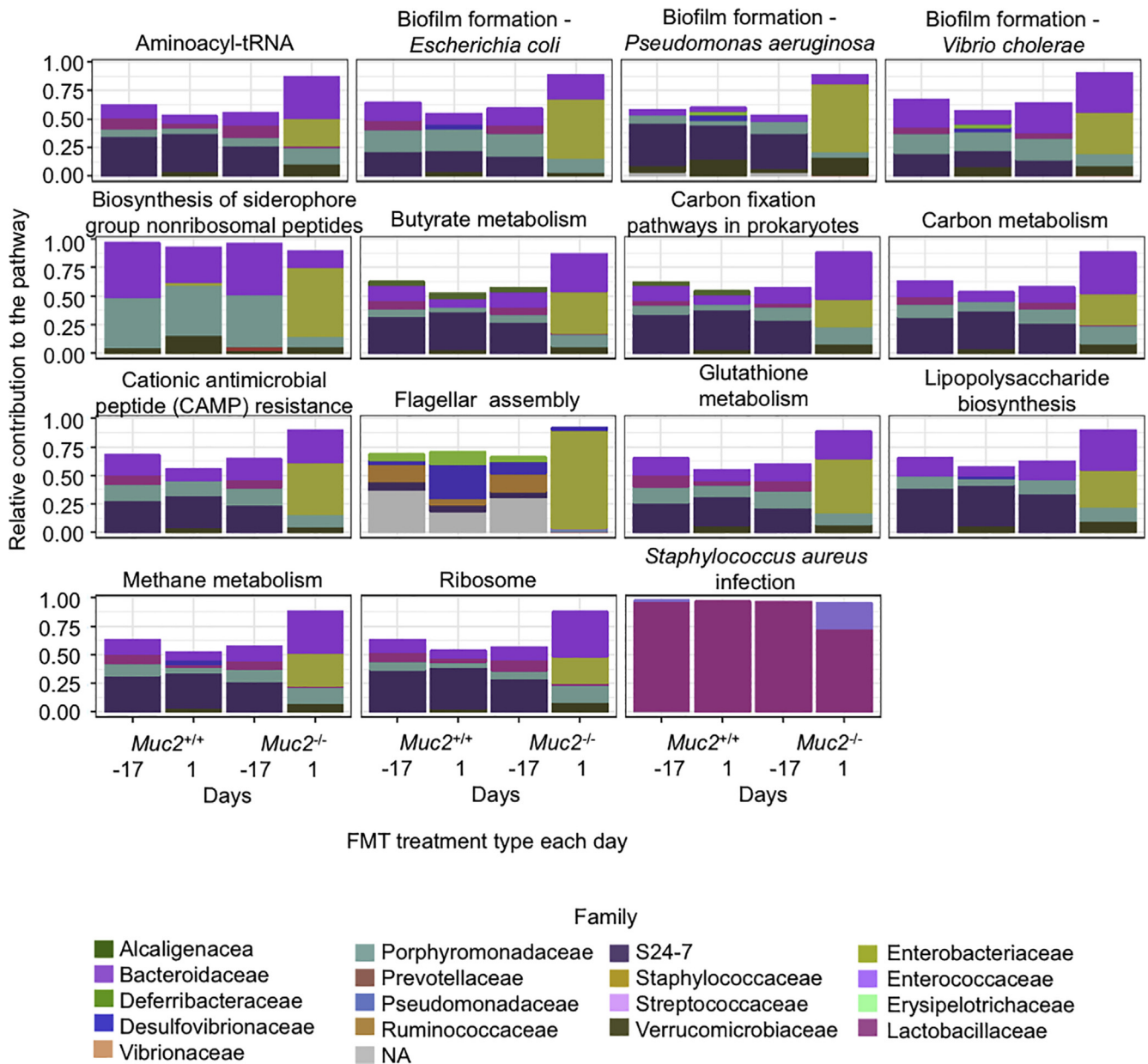


Figure 9. Relative contribution of bacterial families to predicted metagenome in $Muc2^{+/+}$. This figure illustrates the main families that contained the genes involved in the predicted metagenome resulted from PICRUST in $Muc2^{+/+}$ mice FMT with homologous or $Muc2^{-/-}$ microbiota. Bacteria family contribution to PICRUST-predicted pathways are significantly different between $Muc2^{+/+}$ FMT with $Muc2^{-/-}$ or with homologous microbiota. Day -17: untreated control, day 1: 1 day after the last FMT.

Diversity Analysis

Downstream analysis was done in R 3.3.1⁵⁸ using phyloseq 1.16.2⁵⁹ and vegan 2.4-1.⁶⁰ Mitochondrial and chloroplast sequences were removed along with OTUs that appeared only in 1 sample. Samples with <1000 sequences were also removed from the analysis. Alpha-diversity was measured using the Shannon index.⁶¹ Differences in alpha diversity between groups was tested using a Wilcoxon rank sum test, controlling the false discovery rate⁶² and using a cutoff of $P < .05$ for rejecting the null hypothesis of no difference between groups. Between-sample diversity was

evaluated using the Bray-Curtis distance metric on proportionally normalized OTU counts and visualized with nonmetric multidimensional scaling. The generalized linear model framework as implemented in DESeq2⁶³ was used to identify OTUs in the $Muc2^{+/+}$ group at that were differentially abundant between $Muc2^{+/+}$ and $Muc2^{+/+}$ FMT-treated at day 1, controlling for differences at day 0. This approach appropriately control animals for over-dispersed data and variable library sizes.⁶⁴ A P value cutoff of .05 was specified for rejecting the null hypothesis of no difference between groups.

Table 2. Primer Sequences Used for Quantitative Real-Time Polymerase Chain Reaction

Name	Sequence 5' 3'	Annealing temperature (°C)	Reference
16s V6	Fwd: AGGATTAGATACCCTGGTA Rev: CRRACAGAGCTGACGAC	55	23
IL-1 β	Fwd: GCCTCGTGCTGTCGGACCCA Rev: CTGCAGGGTGGGTGTGCCGT	65	20
TNF- α	Fwd: ATGAGCACAGAAAGCATGATC Rev: TACAGGCTTGCTCACTCGAATT	56	73
IFN- γ	Fwd: TCAAGTGGCATAGATGTGGAAGAA Rev: TGGCTCTGCAGGATTTTCATG	54	73
Occludin	Fwd: AGAGGCTATGGGACAGGGCTCTTTGG Rev: CCAACAGGAAGCCTTTGGCTGCTCTTGG	60	74
Claudin-2	Fwd: CCTCGCTGGCTTGATTATCTCTG Rev: GAGTAGAAGTCCCGAAGGA	60	74
Actin	Fwd: CTACAATGAGCTGCGTGTG Rev: TGGGGTGTGAAGGTCTC	54	20

IFN, interferon; IL, interleukin; TGF, transforming growth factor.

Metagenome Predictions

Metagenomes were predicted using PICRUSt 1.1.2³² using a closed reference based OTU table constructed with QIIME 1.9 using the “pick_closed_reference_otus.py” script with default settings.⁶⁵ Gene predictions were generated for KEGG (Kyoto Encyclopedia of Genes and Genomes) orthologs and these predictions were then used as input for HUMAnN2, which was used to calculate taxonomic contribution to functions. Log₂ fold-changes between *Muc2*^{+/+} and *Muc2*^{+/+} FMT-treated at Day1 (same model as for the OTU data) were estimated with DESeq2 and used to identify enriched pathways with gene set enrichment analysis⁶⁶ as implemented in clusterProfiler 3.2.14.⁶⁷

DNA Extraction and 16S rRNA Gene Sequencing

DNA extraction of fecal samples or tissues were carried out using a previously described protocol that enhanced DNA recovery from microbial communities with modifications⁶⁸ to increase quantitative recovery of bacteria across different taxa (enzymatic pretreatment with mutanolysin, lysozyme, and proteinase K). Paired end reads of the V3 region of the 16S rRNA gene using bar coded Illumina sequencing as described previously⁶⁹ with the modification that barcodes are included in the forward primer. A total of 250 nucleotides paired-end sequencing were carried out on a MiSeq Illumina sequencer (Illumina, San Diego, CA) providing complete overlapping sequence reads of the V3. These overlaps are used for correcting poor quality base calls and increasing sequencing accuracy. A total of 30–60,000 16s rRNA reads were generated per sample.

Intestinal Permeability

FITC dextran was used to examine intestinal permeability. Briefly, mice were gavaged with 8-mg FITC-dextran (3–5 kDa; Sigma Aldrich, St Louis, MO); 3 hours later, mice were anaesthetized by isoflurane (Pharmaceutical

Partners of Canada, Richmond Hill, Ontario, Canada), and blood was collected by cardiac puncture and animals sacrificed by cervical dislocation. Whole blood was allowed to clot in the dark for 3 hours at room temperature and centrifuged at 10,000 *g* for 10 min. Serum was transferred to a clean Eppendorf tube and diluted with an equal volume of phosphate-buffered saline. An aliquot of 100 μ L of each sample was loaded onto a black bottom 96-well plate in duplicate, and fluorescence was determined with a plate reader (absorption 485 nm, emission 535 nm). This magnitude is expressed in relative fluorescence units.

Histology and Staining

At the endpoint of the experiments, animals were anesthetized and sacrificed by cervical dislocation and the colon was excised. The colon was opened longitudinally along the mesenteric border and rolled distal to proximal end to form a Swiss roll. The Swiss roll was sectioned in half with one portion being used for histological analysis and the other one used for gene expression analysis. For histology, colonic tissues were fixed in Carnoy's solution, and embedded in paraffin blocks. The 7- μ m tissue sections were rehydrated through an ethanol gradient to water and stained with hematoxylin and eosin (EMD Chemicals, Gibbstown, NJ) to examine overall tissue morphology and Periodic acid Schiff's reagent (PAS; Sigma-Aldrich) to visualize neutral mucins. Histologic score was measured as previously described.²²

Bacterial Localization

Fluorescence in situ hybridization was performed as described previously.⁷⁰ Briefly 5 μ m sliced Carnoy's fixed tissue was incubated with the total bacteria probe EUB338 5'-GCT GCC TCC CGT AGG AGT-3' ([50 ng/ μ L]) coupled with Quasar 670 dye at 46°C overnight. FITC coupled-*Ulex europaeus* agglutinin was used at [1:1000] to visualize the fucosylated residues in mucins and DAPI [1:1000] (Life

Technologies, Carlsbad, CA) for nuclear counterstain. Tissue sections were visualized using an Olympus FV1000 scanning confocal inverted microscope (Olympus, Tokyo, Japan).

Gene Expression Analysis

Total RNA was isolated from snap-frozen tissue using the Trizol reagent method (Invitrogen; Life Technologies) as per manufacturer's specifications, and the yield and purity determined by the ratio of absorbance at 260/280 nm (NanoDrop; Thermo Fisher Scientific, Waltham, MA); only samples with a ratio of ~ 1.8 for DNA and ~ 2.0 for RNA were used. RNA from DSS-treated mice tissue was reprecipitated with lithium chloride precipitation solution⁷¹ (Ambion; Life Technologies). Complementary DNA (cDNA) was prepared using a qScript cDNA synthesis kit. Real-time quantitative polymerase chain reaction was performed using a Rotor Gene 3000 real-time polymerase chain reaction system (Corbett Research, Sydney, Australia). Each reaction mixture contained 100 ng of cDNA, SYBR Green polymerase chain reaction Master Mix (Qiagen, Hilden, Germany), and 1 μ M of primers. A complete list of the primer sequences and conditions used are listed in Table 2. The results were analyzed using the $2^{-\Delta\Delta CT}$ method and expressed as fold changes.

In Vivo IL-10 and TGF- β Neutralization

Muc2^{+/+} and *Muc2*^{-/-} littermates received intraperitoneally 500 μ g of each antibody: anti-TGF- β (BioXcell, BE0057) and anti-IL-10R (BioXcell, BE0050). Mice were sacrificed 5 days postinjection and colon and serum were collected for colitis inflammatory parameters assessment. Mice were weighted every 24 hours and monitored throughout the duration of the experiment.

Myeloperoxidase Assay

Myeloperoxidase activity in mouse colon samples (50 mg of fresh-frozen tissues) was measured as a marker for neutrophil influx as previously described.¹⁷ Briefly, tissue was homogenized in 0.5% hexadecyltrimethylammonium bromide in 50-mM phosphate buffer (pH 6.0). Homogenized tissue was freeze-thawed 3 times, sonicated, and centrifuged (10,000 *g* for 10 minutes at 4°C) and supernatant was collected. The reaction was initiated by addition of 1-mg/mL dianisidine dihydrochloride (Sigma-Aldrich) and 1% H₂O₂, change in optical density was measured at 450 nm.

LPLs Isolation

Animals were euthanized at the end of the experiment, and the colon was surgically removed to isolate LPLs using an established protocol.⁷² In brief, colon was longitudinally cut open and cleaned for any fecal matter using HBSS. Then, it was cut into small 2- to 3-cm pieces to dissociate epithelial cells using Hank's Balance Salt Solution containing EDTA and DTT in a 50-mL falcon tube and placed in an incubator shaker at 37°C for 20 minutes. Supernatant was discarded and remaining tissue was digested with collagenase to obtain LPLs.

Generation of Bone Marrow Chimeric Animals

A single dose of 9.50 Gy was given to *Muc2*^{-/-} and *Muc2*^{+/+} littermates 6–8 weeks old and reconstituted with 5×10^5 bone marrow cells per animal within 5 hours intravenously. Animals were given 2-g/L neomycin sulfate ad libitum for 3 weeks and then intestinal microbiota was reconstituted using FMT. FMT were done 3 times 3 days apart and experiments were carried out 10 days after last FMT.

Flow Cytometry

LPLs were isolated and stimulated with Phorbol 12-myristate 13-acetate and ionomycin in the presence of brefeldin and monensin for 4 h at 37°C in a humidified CO₂ incubator. Stimulated cells were stained for surface antigens with fluorescently labelled antibodies. Cells were then stained with fixable viability dye FV510 for live/dead discrimination followed by intracellular staining using Fix/Perm transcription factor kit (BD Biosciences, Franklin Lakes, NJ) and fluorescently labeled antibodies as follows: IL4 - PE-Cy7 (560699; BD Pharmingen, Franklin Lakes, NJ), KLRG1 - PerCP-Cy5.5 (563595; BD Pharmingen), IL22 - PE (BD Pharmingen; 516404), IFN γ - APC-Cy7 (561479; BD Pharmingen), Ly6G- FITC (BD Pharmingen; 561105), NK1.1 -FITC (561082; BD Pharmingen), CD3- FITC (561798; BD Pharmingen), CD19- FITC (BD Pharmingen; 561740), B220-FITC (561877; BD Pharmingen), NKp46- AF700 (561169; BD Pharmingen), ROR γ t- AF647 (562682; BD Pharmingen), viability dye FV510- BV510 (BD Pharmingen; 564406), CD127- BV421 (566377; BD Pharmingen), and CD45-BV786 (565477; BD Pharmingen). For Tregs quantification, Mouse Th17/Treg Phenotyping Kit (BD Biosciences) was used. Data were acquired on BD FACSCanto flow cytometer and analyzed using FlowJo software (FlowJo, Ashland OR).

Statistical Analysis

Data were analyzed using GraphPad Prism 6 (GraphPad Software, San Diego, CA) for all statistical analysis. Treatment groups were compared using analysis of variance when more than 2 groups were compared. Student's *t* test was used when only 2 groups were compared. Statistical significance was assumed at *P* < .05. Error bars in all the graphs represent mean \pm SEM.

References

- O'Hara AM, Shanahan F. The gut flora as a forgotten organ. *EMBO Rep* 2006;7:688–693.
- Jandhyala SM, Talukdar R, Subramanyam C, Vuyyuru H, Sasikala M, Reddy DN. Role of the normal gut microbiota. *World J Gastroenterol* 2015;21:8787–8803.
- Palm NW, de Zoete MR, Flavell RA. Immune–microbiota interactions in health and disease. *Clin Immunol* 2015; 159:122–127.
- Guarner F. Decade in review—gut microbiota: The gut microbiota era marches on. *Nat Rev Gastroenterol Hepatol* 2014;11:647–649.
- Peterson CT, Sharma V, Elmén L, Peterson SN. Immune homeostasis, dysbiosis and therapeutic modulation of the gut microbiota. *Clin Exp Immunol* 2015;179:363–377.

6. Franzosa EA, Huang K, Meadow JF, Gevers D, Lemon KP, Bohannan BJM, Huttenhower C. Identifying personal microbiomes using metagenomic codes. *Proc Natl Acad Sci* 2015;112:E2930–E2938.
7. The Human Microbiome Project. Structure, function and diversity of the healthy human microbiome. *Nature* 2012;486(7402):207–214.
8. Marchesi JR, Adams DH, Fava F, Hermes GDA, Hirschfield GM, Hold G, Quraishi MN, Kinross J, Smidt H, Tuohy KM, Thomas LV, Zoetendal EG, Hart A. The gut microbiota and host health: a new clinical frontier. *Gut* 2016;65:330–339.
9. Carding S, Verbeke K, Vipond DT, Corfe BM, Owen LJ. Dysbiosis of the gut microbiota in disease. *Microb Ecol Health Dis* 2015;26:26191.
10. Ferreira CM, Vieira AT, Vinolo MAR, Oliveira F a, Curi R, Martins FDS. The central role of the gut microbiota in chronic inflammatory diseases. *J Immunol Res* 2014;1:1–12.
11. Frank DN, St Amand AL, Feldman RA, Boedeker EC, Harpaz N, Pace NR. Molecular-phylogenetic characterization of microbial community imbalances in human inflammatory bowel diseases. *Proc Natl Acad Sci* 2007;104:13780–13785.
12. Ott SJ, Musfeldt M, Wenderoth DF, Hampe J, Brant O, Folsch UR, Timmis KN, Schreidber S. Reduction in diversity of the colonic mucosa associated bacterial microflora in patients with active inflammatory bowel disease. *Gut* 2004;53:685–693.
13. Johansson MEV, Sjövall H, Hansson GC. The gastrointestinal mucus system in health and disease. *Nat Rev Gastroenterol Hepatol* 2013;10:352–361.
14. Johansson MEV, Gustafsson JK, Holmen-Larsson J, Jabbar KS, Xia L, Xu H, Ghishan FK, Carvalho FA, Gewirtz AT, Sjövall H, Hansson GC. Bacteria penetrate the normally impenetrable inner colon mucus layer in both murine colitis models and patients with ulcerative colitis. *Gut* 2014;63:281–291.
15. Palmela C, Chevarin C, Xu Z, Torres J, Sevrin G, Hirten R, Barnish N, Ng SC, Colombel J-F. Adherent-invasive *Escherichia coli* in inflammatory bowel disease. *Gut* 2018;67:574–587.
16. Johansson ME. Mucus layers in inflammatory bowel disease. *Inflamm Bowel Dis* 2014;20:2124–2131.
17. Kumar M, Kisoos-Singh V, Leon-Coria A, Moreau F, Chadee K. The probiotic mixture VSL#3 reduces colonic inflammation and improves intestinal barrier function in *Muc2* mucin deficient mice. *Am J Physiol Gastrointest Liver Physiol* 2017;312:G34–G45.
18. Melo-Gonzalez F, Fenton TM, Forss C, Smedley C, Goenka A, MacDonald AS, Thornton DJ, Travis MA. Intestinal mucin activates human dendritic cells and IL-8 production in a glycan-specific manner. *J Bio Chem* 2018;293:8543–8553.
19. Geva-Zatorsky N, Sefik E, Kua L, Pasman L, Tan TG, Ortiz-Lopez A, Yanortsang TB, Yang L, Jupp R, Mathis D, Benoist C, Kasper DL. Mining the human gut microbiota for immunomodulatory organisms. *Cell* 2017;168:928–943.
20. Kisoos-Singh V, Moreau F, Trusevych E, Chadee K. *Entamoeba histolytica* exacerbates epithelial tight junction permeability and proinflammatory responses in *Muc2*^{-/-} mice. *Am J Pathol* 2013;182:852–865.
21. Bergstrom KSB, Kisoos-Singh V, Gibson DL, Ma C, Montero M, Sham HP, Ryz N, Huang T, Velcich A, Finley BB, Chadee K, Vallance BA. *Muc2* Protects against lethal infectious colitis by disassociating pathogenic and commensal bacteria from the colonic mucosa. *PLoS Pathog* 2010;6:e1000902.
22. Van der Sluis M, De Koning BaE, De Bruijn ACJM, Velcich A, Meijerink JPP, Van Goudoever JB, Buller HA, Dekker J, Van Seuning I, Renes IB, Einerhand AWC. *Muc2*-deficient mice spontaneously develop colitis, indicating that MUC2 is critical for colonic protection. *Gastroenterology* 2006;131:117–129.
23. Reikvam DH, Erofeev A, Sandvik A, Grcic V, Jahnsen FL, Gaustad P, McCoy KD, Macpherson AJ, Meza-Zepeda LA, Johansen F-E. Depletion of murine intestinal microbiota: effects on gut mucosa and epithelial gene expression. *PLoS One* 2011;6:e17996.
24. Wang F, Graham WV, Wang Y, Witkowski ED, Schwarz BT, Turner JR. Interferon-gamma and tumor necrosis factor-alpha synergize to induce intestinal epithelial barrier dysfunction by up-regulating myosin light chain kinase expression. *Am J Pathol* 2005;166:409–419.
25. Pott J, Hornef M. Innate immune signalling at the intestinal epithelium in homeostasis and disease. *EMBO Rep* 2012;13:684–698.
26. Nicholson JK, Holmes E, Kinross J, Burcelin R, Gibson G, Jia W, Pettersson S. Host-gut microbiota metabolic interactions. *Science* 2012;336:1262–1267.
27. Honda K, Littman DR. The microbiota in adaptive immune homeostasis and disease. *Nature* 2016;535:75–84.
28. Sovran B, Loonen LMP, Lu P, Lu P, Hugenholtz F, Belzer C, Stolte EH, Boekschoten MV, Van Baarlen P, Kleerebezem M, de Vos P, Dekker J, Renes IB, Wells JM. IL-22-STAT3 pathway plays a key role in the maintenance of ileal homeostasis in mice lacking secreted mucus barrier. *Inflamm Bowel Dis* 2015;21:531–542.
29. Natividad JM, Pinto-Sanchez MI, Galipeau HJ, Jury J, Jordana M, Reinisch W, Collins SM, Bercik P, Surette MG, Emma-Vercoe E, Verdu EF. Ecobiotherapy rich in firmicutes decreases susceptibility to colitis in a humanized gnotobiotic mouse model. *Inflamm Bowel Dis* 2015;21:1883–1893.
30. Brandl K, Sun L, Neppl C, Siggs OM, Le Gall SM, Tomisato W, Li X, Du X, Maennel DN, Blobel CP, Beutler B. MyD88 signaling in nonhematopoietic cells protects mice against induced colitis by regulating specific EGF receptor ligands. *Proc Natl Acad Sci* 2010;107:19967–19972.
31. Wenzel UA, Jonstrand C, Hansson GC, Wick MJ. CD103⁺CD11b⁺ dendritic cells induce Th17 T Cells in *Muc2*-deficient mice with extensively spread colitis. *PLoS One* 2015;10:e0130750.
32. Langille MGI, Zaneveld J, Caporaso JG, McDonald D, Knights D, Reyes JA, Clemente JC, Burkepille DE, Vega RL, Thurber V, Knight R, Beiko RG, Huttenhower C. Predictive functional profiling of microbial communities using 16S rRNA marker gene sequences. *Nat Biotechnol* 2013;31:814–821.

33. Camilleri M, Madsen K, Spiller R, Van Meerveld BG, Verne GN. Intestinal barrier function in health and gastrointestinal disease. *Neurogastroenterol Motil* 2012; 24:503–512.
34. Atreya R, Neurath MF. IBD pathogenesis in 2014: Molecular pathways controlling barrier function in IBD. *Nat Rev Gastroenterol Hepatol* 2014;12:67–68.
35. Wlodarska M, Kostic AD, Xavier RJ. An integrative view of microbiome-host interactions in inflammatory bowel diseases. *Cell Host Microbe* 2015;17:577–591.
36. Matsuoka K, Kanai T. The gut microbiota and inflammatory bowel disease. *Semin Immunopathol* 2015; 37:47–55.
37. Rankin LC, Girard-Madoux MJH, Seillet C, Mielke LA, Kerdiles Y, Fenis A, Wieduwild E, Putoczki T, Mondot S, Lantz O, Demon D, Papenfuss AT, Smyth GK, Lamkanfi M, Carotta S, Renaud J-C, Shi W, Carpentier S, Soos T, Arendt C, Ugolini S, Huntington ND, Belz GT, Vivier E. Complementarity and redundancy of IL-22-producing innate lymphoid cells. *Nat Immunol* 2016;17:179–186.
38. Sano T, Huang W, Hall JA, Yang Y, Chen A, Gavzy SJ, Lee J-Y, Ziel JW, Miraldi ER, Domingos AI, Bonneau R, Littman DR. An IL-23R/IL-22 circuit regulates epithelial serum amyloid A to promote local effector Th17 responses. *Cell* 2015;163:381–393.
39. Geremia A, Arancibia-Cárcamo CV. Innate lymphoid cells in intestinal inflammation. *Front Immunol* 2017;8:1296.
40. Turner J, Stockinger B, Helmsby H. IL-22 mediates goblet cell hyperplasia and worm expulsion in intestinal helminth infection. *PLoS Pathog* 2013;9:1–7.
41. Geuking MB, Köller Y, Rupp S, McCoy KD. The interplay between the gut microbiota and the immune system. *Gut Microbes* 2014;5:411–418.
42. Wu GD, Bushman FD, Lewis JD. Diet, the human gut microbiota, and IBD. *Anaerobe* 2013;24:117–120.
43. Persson EK, Scott CL, Mowat AM, Agace WW. Dendritic cell subsets in the intestinal lamina propria: ontogeny and function. *Eur J Immunol* 2013;43:3098–3107.
44. Scott CL, Aumeunier AM, Mowat AM. Intestinal CD103+ dendritic cells: master regulators of tolerance? *Trends Immunol* 2011;32:412–419.
45. Iredell J, Brown J, Tagg K. Antibiotic resistance in Enterobacteriaceae: mechanisms and clinical implications. *BMJ* 2015;351:h6420.
46. England Public Health. Investigation of Enterobacteriaceae 2015;4:1–34.
47. Sovran B, Lu P, Loonen L, Hugenholtz F, Belzer C, Stolte EH, Boekschoten MV, Van Baarlen P, Smidt H, Kleerebezem M, de Vos P, Renes IB, Wells JM, Dekker J. Identification of commensal species positively correlated with early stress responses to a compromised mucus barrier. *Inflamm Bowel Dis* 2016;22:826–840.
48. Geerlings SY, Kostopoulos I, Vos WM De, Belzer C. *Akkermansia muciniphila* in the human gastrointestinal tract: when, where, and how? *Microorganisms* 2018;6:1–26.
49. Robles Alonso V, Guarner F. Linking the gut microbiota to human health. *Br J Nutr* 2013;109:S21–S26.
50. Lin PW, Nasr TR, Berardinelli AJ, Kumar A, Neish AS. The probiotic *Lactobacillus GG* may augment intestinal host defense by regulating apoptosis and promoting cytoprotective responses in the developing murine gut. *Pediatr Res* 2008;64:511–516.
51. Johansson MEV, Jakobsson HE, Holmén-Larsson J, Schutte A, Ermund A, Rodriguez-Pineiro AM, Arike L, Wising C, Svensson F, Backhed F, Hansson GC. Normalization of host intestinal mucus layers requires long-term microbial colonization. *Cell Host Microbe* 2015;18:582–592.
52. Joo H-S, Otto M. Molecular basis of in-vivo biofilm formation by bacterial pathogens. *Chem Biol* 2013; 19:1503–1513.
53. Martin M. Cutadapt removes adapter sequences from high-throughput sequencing reads. *EMBnet.journal* 2011;17:10.
54. Edgar RC. UPARSE: highly accurate OTU sequences from microbial amplicon reads. *Nat Methods* 2013; 10:996–998.
55. Edgar RC, Flyvbjerg H. Error filtering, pair assembly and error correction for next-generation sequencing reads. *Bioinformatics* 2015;31:3476–3482.
56. Wang Q, Garrity GM, Tiedje JM, Cole JR. Naive bayesian classifier for rapid assignment of rRNA sequences into the new bacterial taxonomy. *Appl Environ Microbiol* 2007;73:5261–5267.
57. Köster J, Rahmann S. Snakemake — a scalable bioinformatics workflow engine. *Bioinformatics* 2012; 28:2520–2522.
58. R Development Core Team. R: a language and environment for statistical computing; 2011.
59. McMurdie PJ, Holmes S. Phyloseq: An R package for reproducible interactive analysis and graphics of microbiome census data. *PLoS One* 2013;8:e61217.
60. Oksanen AJ, Blanchet FG, Friendly M, Kindt R, Legendre P, McGlenn D, Minchin PR, O'Hara RB, Simpson GL, Solymos P, Stevens MHH, Szoecs E, Wagner H. Package 'vegan' 2015.
61. Shannon CE. A mathematical theory of communication 1948;27:379–423.
62. Benjamini Y, Hochberg Y. Controlling the false discovery rate: a practical and powerful approach to multiple testing. *J R Stat Soc Ser B* 1995;57:289–300.
63. Love MI, Huber W, Anders S. Moderated estimation of fold change and dispersion for RNA-seq data with DESeq2. *Genome Biol* 2014;15:1–21.
64. McMurdie PJ, Holmes S. Waste not, want not: why rarefying microbiome data is inadmissible. *PLOS Comput Biol* 2014;10:e1003531.
65. Caporaso JG, Kuczynski J, Stombaugh J, Bittinger K, Bushman FD, Costello EK, Fierer N, Pena AG, Goodrich JK, Gordon JI, Huttley GA, Kelly ST, Knights D, Koenig JE, Ley RE, Lozupone CA, McDonald D, Muegge BD, Pirrung M, Reeder J, Sevinsky JR, Turnbaugh PJ, Walters WA, Widmann J, Yatsunenko T, Zaneveld J, Knight R. QIIME allows analysis of high-throughput community sequencing data. *Nat Methds* 2010;7:335–336.
66. Subramanian A, Tamayo P, Mootha VK, Mukherjee S, Ebert BL, Gillette MA, Paulovich A, Pomeroy SL, Golub TR, Lander ES, Mesirov JP. Gene set

- enrichment analysis: A knowledge-based approach for interpreting genome-wide. *Pro Nat Aca Sci* 2005; 102:15545–15550.
67. Yu G, Wang L-G, Han Y, He Q-Y. clusterProfiler: an R package for comparing biological themes among gene clusters. *Omi A J Integr Biol* 2012;16:284–287.
 68. Whelan FJ, Verschoor CP, Stearns JC, Rossi L, Luinstra K, Loeb M, Smieja M, Johstone J, Surette MG, Bowdish DM. The loss of topography in the microbial communities of the upper respiratory tract in the elderly. *Ann Am Thorac Soc* 2014;11:513–521.
 69. Bartram AK, Lynch MDJ, Stearns JC, Moreno-Hagelsieb G, Neufeld JD. Generation of multimillion-sequence 16S rRNA gene libraries from complex microbial communities by assembling paired-end Illumina reads. *Appl Environ Microbiol* 2011;77:3846–3852.
 70. Johansson MEV, Hansson GC. Preservation of mucus in histological sections, immunostaining of mucins in fixed tissue, and localization of bacteria with FISH. In: *Mucins: Methods and Protocols*, 842; 2012:229–235.
 71. Viennois E, Chen F, Laroui H, Baker MT, Merlin D. Dextran sodium sulfate inhibits the activities of both polymerase and reverse transcriptase: Lithium chloride purification, a rapid and efficient technique to purify RNA. *BMC Res Notes* 2013;6:360.
 72. Weigmann B, Tubbe I, Seidel D, Nicolaev A, Becker C, Neurath MF. Isolation and subsequent analysis of murine lamina propria mononuclear cells from colonic tissue. *Nat Protoc* 2007;2:2307–2311.
 73. Giulietti a, Overbergh L, Valckx D, Decallonne B, Bouillon R, Mathieu C. An overview of real-time quantitative PCR: applications to quantify cytokine gene expression. *Methods* 2001;25:386–401.
 74. Roxas JL, Koutsouris A, Bellmeyer A, Tesfay S, Royan S, Falzari K, Harris A, Cheng H, Rhee KJ, Hecht G. Enterohemorrhagic *E. coli* alters murine intestinal epithelial tight junction protein expression and barrier function in Shiga toxin independent manner. *Lab Invest* 2010;90:1152–1168.

Received November 8, 2019. Accepted July 7, 2020.

Correspondence

Address correspondence to: Kris Chadee, PhD, Cumming School of Medicine, Department of Microbiology, Immunology and Infectious Diseases, University of Calgary Health Sciences Centre, 3330 Hospital Drive NW, Calgary, Alberta T2N 4N1, Canada. e-mail: kchadee@ucalgary.ca; fax: (403) 270-2772.

Acknowledgments

The authors thank Pina Colarusso and Rima-Marie Wazen from the Live Cell Imaging Facility at the Snyder Institute for technical assistance.

CRediT Authorship Contributions

Aralia Leon Coria (Conceptualization: Equal; Formal analysis: Lead; Investigation: Lead; Methodology: Supporting; Validation: Supporting; Writing – original draft: Lead; Writing – review & editing: Supporting)

Manish Kumar (Conceptualization: Supporting; Formal analysis: Supporting; Investigation: Supporting; Methodology: Supporting; Validation: Supporting; Visualization: Supporting; Writing – original draft: Supporting)

Matthew Workentine (Data curation: Supporting; Formal analysis: Lead; Software: Lead; Validation: Supporting)

France Moreau (Formal analysis: Supporting; Investigation: Supporting; Project administration: Supporting; Resources: Lead; Validation: Supporting)

Michael Surette (Data curation: Lead; Formal analysis: Supporting; Methodology: Supporting; Software: Supporting; Validation: Supporting)

Kris Chadee (Conceptualization: Equal; Funding acquisition: Lead; Project administration: Lead; Supervision: Lead; Validation: Equal; Writing – review & editing: Equal)

Conflicts of interest

The authors disclose no conflicts.

Funding

Operating grants from Crohn's and Colitis Canada and the Canadian Institute of Health Research supported this work. Aralia Leon-Coria was supported by scholarships from CONACyT and NSERC-CREATE.